

***NCHRP IDEA Program***

---

# **Development of an Innovative Bio-Mediated Self-Healing Concrete Technology**

Final Report for  
NCHRP IDEA Project 233

Prepared by:  
Xiong (Bill) Yu  
Case Western Reserve University

***July 2023***

---

NATIONAL  
ACADEMIES

Sciences  
Engineering  
Medicine

**TRB** TRANSPORTATION RESEARCH BOARD

## **Innovations Deserving Exploratory Analysis (IDEA) Programs Managed by the Transportation Research Board**

This IDEA project was funded by the NCHRP IDEA Program.

The TRB currently manages the following three IDEA programs:

- The NCHRP IDEA Program, which focuses on advances in the design, construction, and maintenance of highway systems, is funded by American Association of State Highway and Transportation Officials (AASHTO) as part of the National Cooperative Highway Research Program (NCHRP).
- The Safety IDEA Program currently focuses on innovative approaches for improving railroad safety or performance. The program is currently funded by the Federal Railroad Administration (FRA). The program was previously jointly funded by the Federal Motor Carrier Safety Administration (FMCSA) and the FRA.
- The Transit IDEA Program, which supports development and testing of innovative concepts and methods for advancing transit practice, is funded by the Federal Transit Administration (FTA) as part of the Transit Cooperative Research Program (TCRP).

Management of the three IDEA programs is coordinated to promote the development and testing of innovative concepts, methods, and technologies.

For information on the IDEA programs, check the IDEA website ([www.trb.org/idea](http://www.trb.org/idea)). For questions, contact the IDEA programs office by telephone at (202) 334-3310.

IDEA Programs  
Transportation Research Board  
500 Fifth Street, NW  
Washington, DC 20001

The project that is the subject of this contractor-authored report was a part of the Innovations Deserving Exploratory Analysis (IDEA) Programs, which are managed by the Transportation Research Board (TRB) with the approval of the National Academies of Sciences, Engineering, and Medicine. The members of the oversight committee that monitored the project and reviewed the report were chosen for their special competencies and with regard for appropriate balance. The views expressed in this report are those of the contractor who conducted the investigation documented in this report and do not necessarily reflect those of the Transportation Research Board; the National Academies of Sciences, Engineering, and Medicine; or the sponsors of the IDEA Programs.

The Transportation Research Board; the National Academies of Sciences, Engineering, and Medicine; and the organizations that sponsor the IDEA Programs do not endorse products or manufacturers. Trade or manufacturers' names appear herein solely because they are considered essential to the object of the investigation.

## **NCHRP IDEA PROGRAM**

### **COMMITTEE CHAIR**

KEVIN PETE  
*Texas DOT*

### **MEMBERS**

FARHAD ANSARI  
*University of Illinois at Chicago*

AMY BEISE  
*North Dakota DOT*

NATANE BRENNFLECK  
*California DOT*

JAMES “DARRYL” DOCKSTADER  
*Florida DOT*

ERIC HARM  
*Consultant*

SHANTE HASTINGS  
*Delaware DOT*

PATRICIA LEAVENWORTH  
*Massachusetts DOT*

TOMMY NANTUNG  
*Indiana DOT*

DAVID NOYCE  
*University of Wisconsin, Madison*

A. EMILY PARKANY  
*Vermont Agency of Transportation*

TERESA STEPHENS  
*Oklahoma DOT*

JOSEPH WARTMAN  
*University of Washington*

### **AASHTO LIAISON**

GLENN PAGE  
*AASHTO*

### **FHWA LIAISON**

MARY HUIE  
*Federal Highway Administration*

### **TRB LIAISON**

ILONA KASTENHOFER  
*Transportation Research Board*

## **IDEA PROGRAMS STAFF**

RUSSELL HOUSTON  
*Associate Executive Director , Transportation  
Research Board*

WASEEM DEKELBAB  
*Deputy Director, Cooperative Research  
Programs*

SID MOHAN  
*Associate Program Manager*

INAM JAWED  
*Senior Program Officer*

PATRICK ZELINSKI  
*Senior Program Officer*

Mireya Kuskie  
*Senior Program Assistant*

## **EXPERT REVIEW PANEL**

ERIC HARM, *Consultant*

EDWARD GARBOCZI, *National Institute  
of Standards and Technology*

ROBERT SPRAGG, *FHWA*

JULIE BUFFENBARGER, *Beton Consulting  
Engineers, LLC*

WILL GOLD, *American Concrete Institute*

# **Development of an Innovative Bio-Mediated Self-Healing Concrete Technology**

## **NCHRP IDEA Program Final Report**

### **IDEA Project NCHRP-233**

*Prepared for*

The NCHRP IDEA Program  
Transportation Research Board  
National Academies of Sciences, Engineering, and Medicine

*by*

*Xiong (Bill) Yu*

*Case Western Reserve University*

*July 31, 2023*

## Table of Contents

Acknowledgement .....	i
Glossary .....	ii
Executive Summary .....	3
IDEA Product .....	5
Concept and Innovation .....	6
Investigation .....	7
Plans for Implementation.....	45
Conclusions.....	46
Investigators' Profiles.....	47
References .....	48
Appendix: Research Results .....	50

## Acknowledgement

The project was carried out with the assistance of Dr. Xijin (Emma) Zhang, graduate assistant and postdoctoral researcher at Case Western Reserve University, who will become an Assistant Professor at George Mason University in Fall 2023. The project activities were also contributed by Rodrigo Teixeira Schossler and Qammar Abbas, both are Ph.D. students and graduate research assistant.

We appreciate the constructive comments and suggestions to the team from the project expert advisory panel, which include Dr. *Edward J. Garboczi*, Fellow, Applied Chemicals and Materials Division, National Institute of Standards and Technology; Dr. *Robert Spragg*, Concrete Materials Engineer, Federal Highway Administration; Dr. *Julie Buffenbarger*, FACI, LEED AP, Senior Scientist & Sustainability Principal, Beton Consulting Engineers LLC; *Will Gold*, Engineer, the American Concrete Institute (previously Technical Director, Master Builder Chemicals LLC). Our sincere appreciation also goes to project advisor *Eric Harm*, Hanson Professional Service Inc., for the dedicated advisory on the conduct of this project. Specially, we appreciate Mr. *Inam Jawed*, NCHRP-IDEA program officer, for the tireless guidance during this project.

## Glossary

ADA	Americans with Disabilities Act
AI	Artificial Intelligence
API	Application Programing Interface
AVL	Automatic Vehicle Location
BLE	Bluetooth Low Energy
BVIs	Blind and Visually Impaired Individuals
DAU	Driver Alerting Unit
GPS	Global Positioning System
HIPPA	Health Insurance Portability and Accountability Act
IAPB	International Agency for the Prevention of Blindness
IoT	Internet of Things
IT	Information Technology
ITS	Intelligent Transportation Systems
MOD	Mobility on Demand
NCHRP-IDEA	National Cooperative Highway Research Program-Innovation Deserving Exploratory Analyses
RF	Radio Frequency
V2I	Vehicle to Infrastructure

## EXECUTIVE SUMMARY

Cracks in concrete structures significantly compromise their durability. For example, cracks are commonly observed in bridge decks at different stages of service, due to early age volume shrinkage, or long term service loads, and climate conditions (i.e., dry-wet cycles, freeze-thaw cycles). Non-structural cracks generally don't pose immediate safety concern. However, they compromise the service life of bridge decks by allowing water and salt ingress that accelerate rebar and concrete corrosion. Bridge deck rehabilitation and replacement is typically the largest share of bridge maintenance cost during the service period of a highway bridge. The large number of bridges and distributed nature of transportation infrastructure makes it difficult to inspect and treat concrete cracks timely with conventional manual maintenance procedures. Therefore, autogenous healing concrete cracks with no need of human intervention, i.e., self-healing concrete, have unique advantages.

This project aims to conduct proof-of-concept investigation towards developing an innovative fungi-mediated self-healing concrete technology. The innovative self-healing concrete technology developed is microcapsules in the size of sub-millimeter which contains fungi-based self-healing agent. The microcapsules can be introduced into fresh concrete mix as a new type of concrete admixture. From this, fast and autogenous concrete crack healing can be sustained over its service life. The anticipated healing performance includes recovery of the mechanical strength of concrete with fungi-induced biomineralization process; as well as improved water tightness with hydrophobic fungi fiber, which prevents water and deicing salt ingress. The project activities were implemented in three phases following NCHRP-IDEA program guidelines.

Research activities during the *Phase 1* focused on assessing the interactions of fungi with concrete. These aimed to improve fungi survivability and growth, which are crucial to achieve efficient healing functions. From the results of experimental studies, two types of fungi strains with promising healing performance were identified based on their favorable interactions with concrete. The study further developed and evaluated methods to improve the survivability and growth rates of fungi, which were to ensure efficient fungi growth in concrete pore environment.

In *Phase 2*, protection strategies such as encapsulation were developed to protect fungi spores to endure mechanical loads during the concrete mixing process and to help them survive the possible long dormancy period inside the concrete matrix. A scalable procedure has been developed for microcapsule production, which allows streamlined large scale production of self-healing microcapsules.

Research activities in *Stage 3* developed and implemented an experimental protocol to assess the performance of the self-healing agents. Microcapsules containing fungi-based self-healing agent were introduced into the mortar mixture during the mixing process. Specimens with different concentrations of self-healing microcapsules were produced. After a curing period, cracks with a range of widths were generated in the mortar specimens. The results show that cracks over 1mm in a cement mortar mix were successfully healed with the fungi-based healing agents. (It is noted that autogenous healing by hydration of unhydrated cement heals small cracks less than 0.1mm. Documented literature indicates bacteria-based self-healing via microbial induced calcite precipitation (MICP) only heals cracks up to 0.4mm.)

Besides, the surface of crack healed with fungi shows strong hydrophobicity. This will help to mitigate concrete deterioration associated with ionic transport into concrete matrix (i.e., deicer ingress, corrosion, etc.), which would improve the durability.

Overall, this NCHRP-IDEA Type 1 proof-of-concept study successfully validated the technology concept of fungi-based self-healing for concrete. The results indicated that the fungi-based self-healing agents achieved excellent performance. The capability of this new technology in healing wide crack well beyond the current state of art demonstrates significant potentials for engineering applications. Future development and implementation of this innovative technology in transportation applications can significantly improve the longevity of bridge decks and other concrete structures.



## **IDEA PRODUCT**

The product from this study is an innovative fungi-mediated self-healing concrete technology. It is based on production of microcapsule containing fungi-based self-healing agents. The microcapsules can be introduced into fresh concrete mix as a new types of concrete admixture. From this, fast and autogenous concrete crack healing can be sustained over its service life. The healing process lead to hydrophobic concrete surface which prevents water and deicing salt ingress. Results of this NCHRP-IDEA Type 1 (proof-of-concept) project observed superior performance of this new technology in autogenously healing wide crack well beyond the current state of art. Results from this project demonstrates promising potentials of a new self-healing concrete admixture to ensure long lasting transportation structures.

## CONCEPT AND INNOVATION

The proposed self-healing technology leverage fungi growth to rapidly cover the exposed crack surfaces and seal the cracks with fungi-mediated bio-mineralization processes. Besides, the hydrophobic nature of the fungi fiber ensures water tightness and prevents water ingress into cracks. Overall, the technology has potentials to recover the mechanical properties and water tightness of cracked concrete autogenously and fast. Such performance will lead to major savings in cost and labor compared with conventional concrete crack treatment procedures. This innovative autogenously self-healing concrete technology will significantly improve the longevity and performance of bridge decks and other concrete structures.

# INVESTIGATION

## 1. Research Background

Concrete structures are prone to cracking during early stage curing or during the long term aging process [1, 2]. Structural cracks directly impair its load-bearing capacity, while non-structural cracks indirectly affect its service life. Cracks enable easier penetration of liquid and gas containing harmful substances into the concrete matrix. Furthermore, cracking compromises durability through the corrosion of embedded reinforcement and the degradation of concrete integrity [3, 4]. If micro-cracks grow and reach the reinforcement, the ingress of moisture and other impurities such as chloride and sulfate ions in cracks will further react with reinforcements. These chemical reactions generate an internal expansion that cause pressure on the concrete matrix, leading to spalling. Without immediate and proper treatment, cracks are precursors to structural failure and eventually require substantial and costly maintenance and repair [5]. Therefore, the conventional repairing methods pose negative effects on the development of sustainable materials [6]. Impregnation of cracks with epoxy-based or other synthetic fillers consisting of volatile organic compounds results in environmental problems [6]. On the other hand, traditionally man-devised repairing concrete methods not only increase the annual construction budgets [7], but are also time-consuming and lead to reduced productivity [8].

Fungi-mediated technology potentially helps to self-heal cracks in concrete and prolong the service life and concrete bridges. Filamentous fungi are chosen in this project because 1) their enormous surface-to-volume ratio allows considerable interactions with the substrate; 2) filamentous fungi show a quick growth rate, which facilitate fungi to cover wide cracks with the extension of mycelium and spread of spores; 3) cultivating nutrition only contains the ingredient from potatoes, which is cleaner and environmentally friendly.

Therefore, this project explored the use of fungi-mediated technology to self-heal cracks in concrete and to promote its application in transportation assets such as bridge deck or pavement. The project technical explorations employed a three-stage approach. During *the first phase*, a fungal strain capable of thriving in alkaline mortar was identified through experiments. To facilitate the observation of fungal growth behavior, inoculation was carried out on the mortar's surface, allowing for the examination of interactions between the fungi and concrete. Subsequently, during *the second phase*, the efforts concentrated on encapsulated technology, which aimed at enhancing their growth rates and self-healing efficiency in alkaline concrete environments. Finally, *the third phase* entailed an investigation into the self-healing performance by the encapsulated fungi-mediated self-healing technology.

For the convenience of following a logic sequence, the details of investigation activities are organized in the three phases. A summary of the corresponding research tasks is then provided.

## 2. Research Activities

### 2.1 Phase 1: Study of Fungi-Mortar Surface Interactions

In the first stage, the activities focused on the experiments on inoculating fungi on the surface of mortar samples and observing the growth behavior as well as the fungi-mortar surface interactions. From a series of screening assessment, a promising fungi strain were selected from preliminary assessment their interactions with concrete, i.e., fungi *Fusarium oxysporum*.

#### 2.1.1 Experimental design

##### *Mortar specimens preparation*

The mix design of mortar is shown in Table 1, which includes the type I Portland cement (Lafarge®) and fine sand. All the materials used for the experiments (including water and nutrients and utensils) were autoclaved at 120 °C for 15 minutes prior to use. The diameters of the fine sand fall into the range between 0.030 mm and 1mm. Plain mortar specimens were prepared with the water to cement with the mass ratio (w/c) of 0.5 and the sand to cement with mass ratio of 2.46. Water-reducer was used in the mixing process. Upon finishing the mixing procedures, specimens with a 50.8 mm diameter were prepared using standard molds. Slices of mortar specimens with a height of 6 mm were prepared from the plain mortar specimens after 90 days of curing. To eliminate possible contaminants caused by the cutting process, all of the mortar slices

were put in the oven set at 100 °C for two hours. The mortar slices were placed in sterilized Petri dishes with an inner diameter of 53.5 mm.

**Table 1** Proportions of plain mortar mix design used in experiments

Water (g)	Cement (g)	Sand (g)	Water-Reducer (g)	Total (g)
65	130	320	0.39	515.39

### ***Nutrition medium***

Fungi require nutrition to grow. Potato Dextrose Agar (PDA) and Potato Dextrose Broth (PDB) are common types of nutrition medium. PDA is in a semi-solid phase at the room temperature while PDB is in liquid phase. During the trial experiments, it was found that the semi-solid PDA makes it difficult to accurately measure its pH value. PDA was observed to shrink which affected the interactions between the growing fungal mycelium and the mortar. Hence, PDB solution was chosen as a nutrition provider for fungi, which was prepared by dissolving 24 g PDB powder into 1 L deionized water. 10 mL PDB nutrition medium was placed on the top of the mortar slices.

### ***Fungal culture***

The fungi *Fusarium oxysporum* (ATCC MYA-1198) was selected for this study due to its fast growth rates. The fungi strain *Fusarium oxysporum* is a fibrous fungi type. The fungi colony was transferred to the surface of mortar specimens by cutting discs of 5.75 mm diameter from the leading edge of the vendor-supplied fungal colony using a glass cork borer that was flame-sterilized prior to use. The fungal discs were inoculated at the center of the nutrition medium. The Petri dishes were covered with the lid, which minimizes evaporation while allows oxygen supply for the growth of *Fusarium oxysporum*. The mortar specimens with inoculated fungi were cultivated in an incubator at  $29 \pm 1.2$  °C. The growth behaviors of *Fusarium oxysporum* were observed at defined time intervals.

### ***Contrast groups of experimental samples***

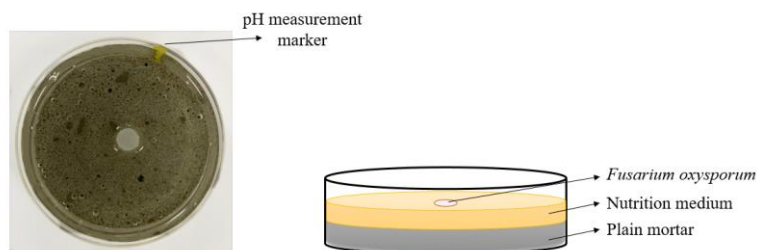
Four different groups of contrast specimens, including one experimental group and three control groups were included in the study. The first group is the nutrition medium without fungi. The second group is nutrition medium and inoculated *Fusarium oxysporum* fungi. The third group is the nutrition medium on mortar slice. The last group is the mortar with nutrition medium and inoculated *Fusarium oxysporum* fungi. Three duplicate samples were prepared for each group. Information about the contrast groups is shown in Table 2. The schematic of the placements is shown in Figure 1. Information, such as the pH value, growth behaviors, etc. are monitored among the contrast groups.

**Table 2** Summary of contrast groups of samples

Group Name*	Number of samples	Mortar (M)	Potato Dextrose Broth (PDB)	<i>Fusarium oxysporum</i> (F)
PDB	3	×	√	×
PDB-F	3	×	√	√
PDB-M	3	√	√	×
PDB-M-F	3	√	√	√

×: without; √: with

\* Name convention: M represents with Mortar, F represents with *Fusarium oxysporum*, number represent the sample No. within the group.



**Fig. 1** Schematic of prepared specimens (Group PDB-M-F)

## 2.1.2 Results

### *Visual observed fungal mycelium growth behaviors*

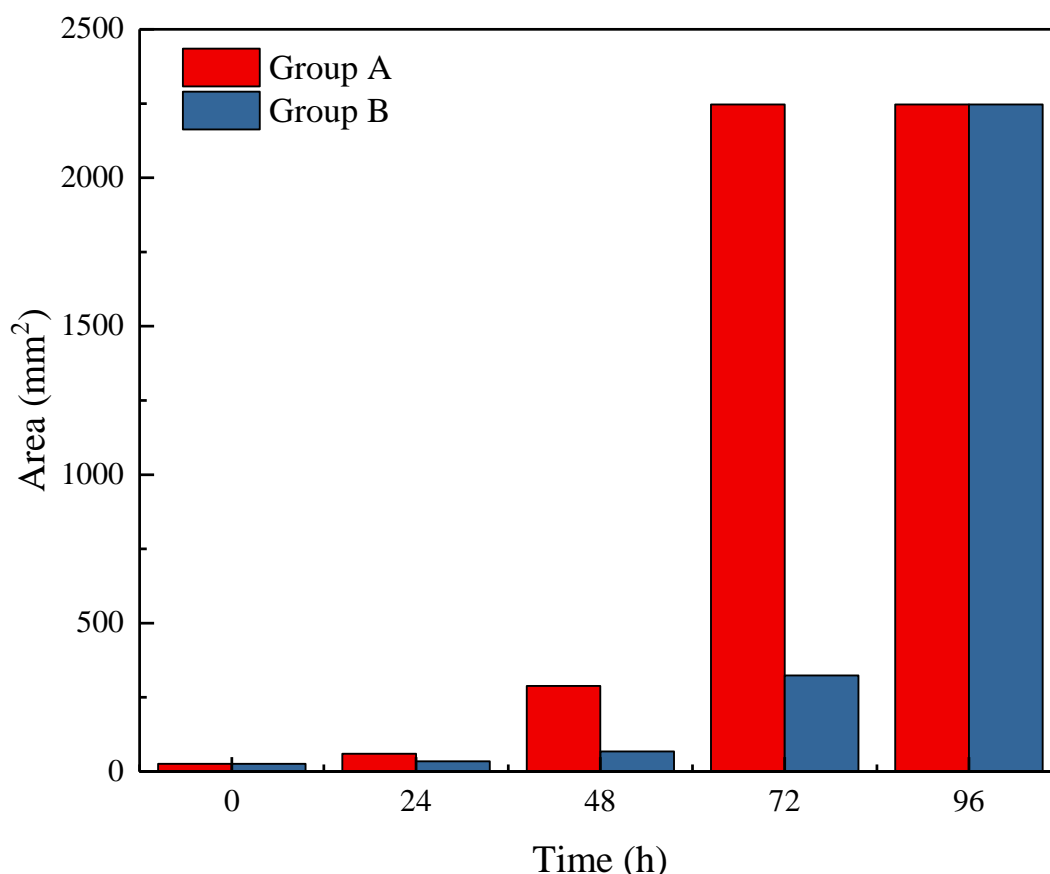
Daily taken photos were utilized to observe the growth behaviors of fungi in different samples. It was observed that the six samples from the two groups with *Fusarium oxysporum* inoculums (PDB-F and PDB-M-F) showed different fungi growth characteristics, including the colony color and mycelial growth pattern. The observed behaviors of fungi in the contrast samples were classified into three groups. Group A include all of the PDB-F samples (i.e., PDB-F1, 2 and 3, PDB with inoculated fungi), in which the fungi colonies were observed to develop vigorously compared with other groups. This set the baseline of fungal growth since PDB provided a favorable environment for fungi to grow. Group B included PDB-M-F2, whose colony was able to grow under the influence of plan mortar. The Group C include PDB-M-F1 and PDB-M-F3, where no obvious growth of mycelium was observed. A representative set of pictures were chosen to show different mycelium growth behaviors in Table 3.

**Table 3** Summary of daily taken pictures in each group

Specimen No.	24 hrs	48 hrs	72 hrs	96 hrs	120 hrs
<b>Group A</b> (PDB-F1,2,3)					
<b>Group B</b> (PDB-M-F2)					
<b>Group C</b> (PDB-M-F1 & 3)					

Table 3 shows that the overall growth rate of mycelium surface area in each group was: Group A > Group B > Group C. The experiments also show seemingly contradictory observations in terms of the growth behaviors of fungi. The mycelium of *Fusarium oxysporum* was able to grow on the surface of mortar in Group B and was not able to grow on the surface of mortar in Group C. Experimental measurements were conducted to provide insight on the underlying mechanism.

The open-source software Image J (<https://imagej.nih.gov/ij/>) was utilized to analyze the fungal surface area from the recorded pictures (Fig. 2). The surface area of the initial fungal inoculum for all the groups were around 25.95 mm<sup>2</sup>. The fungal inoculum germinated in Group A, the area increased to 59.87 mm<sup>2</sup> after 24 hours, while no obvious changes were observed in samples in Group B and Group C. In the next 24 hours (48 hours in total), spores sprouted in various locations in samples in Group A. In the meanwhile, fungal inoculum grew in Group B with the surface area of the mycelium increased to 67.61 mm<sup>2</sup>. After 72 hours, the mycelium of *Fusarium oxysporum* in Group A completely covered the Petri dish with the surface area of 2246.87 mm<sup>2</sup> or 86 times that of the original inoculum. The mycelium grew thicker in the next two days and became stable after 120 hours. For Group B, the mycelium of *Fusarium oxysporum* grew fast between 72 hours and 120 hours. The mycelium covered the whole surface of Petri dish after 96 hours. The ability to rapid grow on the surface of mortar would contribute to high crack healing efficiency. Color of fungi colony varied from white, pink, and purple in groups A and B. Their original inoculum (located at the center) showed pink or purple at the early growing stage. The color of the colonies turned white as the mycelium became thicker. No obvious fungal mycelium occurred in Group C, except white spots were found in Group C and was suspected to be a mixture of calcium hydroxide and fungal hyphae. Microstructural examination was conducted to evaluate the formation of spores in Group C.



**Fig. 2** Surface area in representative sample from Group A and Group B

#### **Monitoring data of pH values in the nutrition medium**

The experimental observations imply that the introduction of mortar slice affected fungal growth behaviors. In general, the growth behaviors of fungi are affected by a few controlling factors, i.e., nutrition, oxygen, pH etc. The contrast samples were designed to study the effects of these important factors affecting the metabolism of fungi. The pH value in the nutrition medium was monitored to investigate the influence of extracellular pH on the growth of *Fusarium oxysporum*.

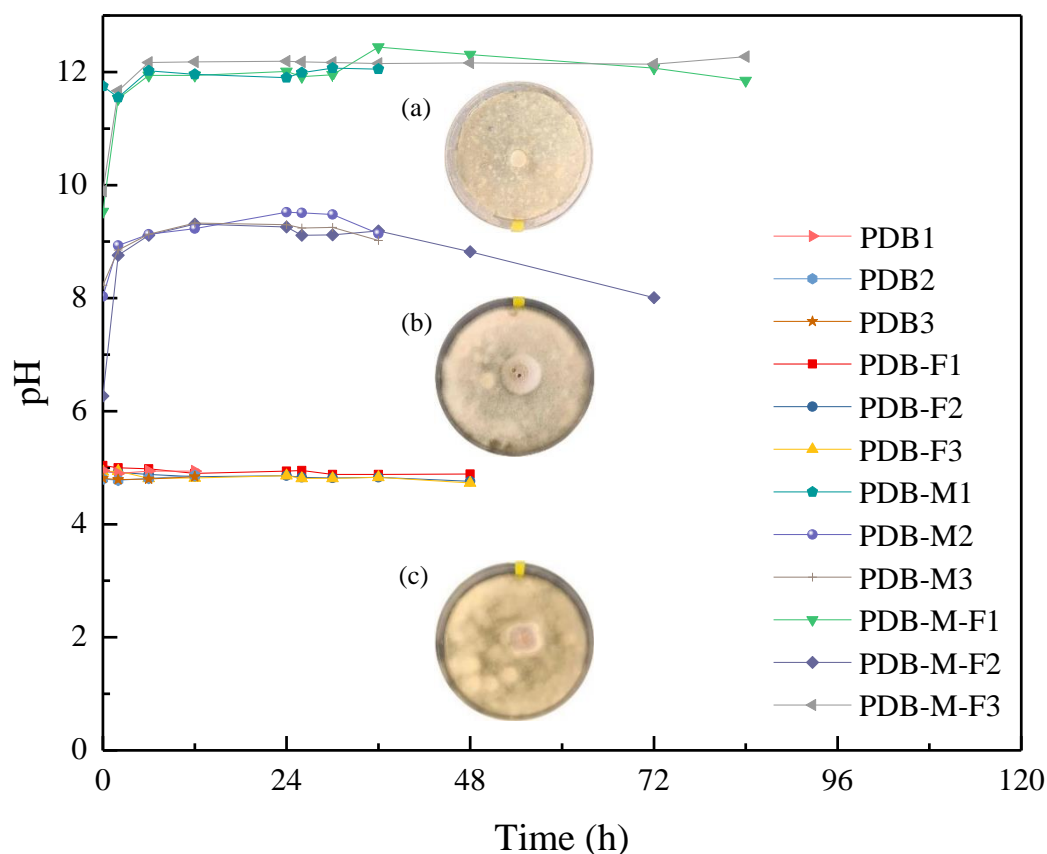
The measured pH value of the original PDB ranged from 4.8 to 5.0. It is known that the hydrating mortar is highly alkaline, which is attributed to the formation of portlandite (calcium hydroxide). Portlandite is the second most common hydration product (after calcium-silica-hydrate) during the hydration of ordinary Portland cement, which leads to increased pH in pores to the range of 11-13 [7]. Therefore, when PDB nutrition medium is in contact with plain mortar, the alkaline

ions in the plain mortar will leachate to the interfaces between plain mortar and nutrition medium. This increases the pH values of the nutrition medium due to the diffusion of calcium hydroxide into PDB medium.

Figure 3 shows the measured evolution of pH values in different specimens and the corresponding images of the surface of the specimens. The contrast groups, PDB and PDB-F, show relatively stable pH values of around 5. The contrast groups, PDB-M and PDB-M-F showed higher initial pH values, possibly because calcium hydrate ions in the plain mortar are leachated into PDB. The exposed surface of mortar slice in contact with the nutrition medium include unhydrated cement, hydrated products including calcium hydrate, and sand particles. The unhydrated cement reacts with water in the nutrition medium which produces alkaline hydrate products, which led to the increase of the pH in the nutrition medium.

The initial pH values were different in different samples, possibly due to the differences in distribution of cement on the surface of cut mortar slices. For PDB-M2, PDB-M3 and PDB-M-F2, more sand and aggregates covering the surface of cut slice led to lower pH; while for PDB-M1, PDB-M-F1 and PDB-M-F3, larger area of cement on the surface of slice resulted in the higher pH.

The observed pH in Figure 3 together with the daily growth behaviors as shown in the photos in Table 3 indicated that the pH in the medium has an important effect on the mycelium growth of *Fusarium oxysporum*. This type of fungi favors an acidic environment, the mycelium of *Fusarium oxysporum* grew more in the samples of Group A. For Group B (PDB-M-F2), the pH value is around 9.2, where mycelium developed and covered the surface of the mortar sample. For Group C, the pH of PDB-M-F1 and PDB-M-F3 increased to 12 after the chemical exchange and no mycelium growth was observed. This indicates that high pH of mortar might inhibit the growth of fungi.



**Fig. 3** Monitored development of pH values of medium in different testing samples: (a) Insignificant mycelium development in the Group C (PDB-M-F1 and PDB-M-F3) with pH of around 12 after 120 hours (b) Mycelium fully developed in Group B (PDB-M-F2) with pH value of around 8-9 after 120 hours (c) Mycelium fully developed in Group A (PDB1, PDB2 and PDB3) with pH of around 5 after 120 hours

### ***Phases of mass change and corresponding fungi mycelium development***

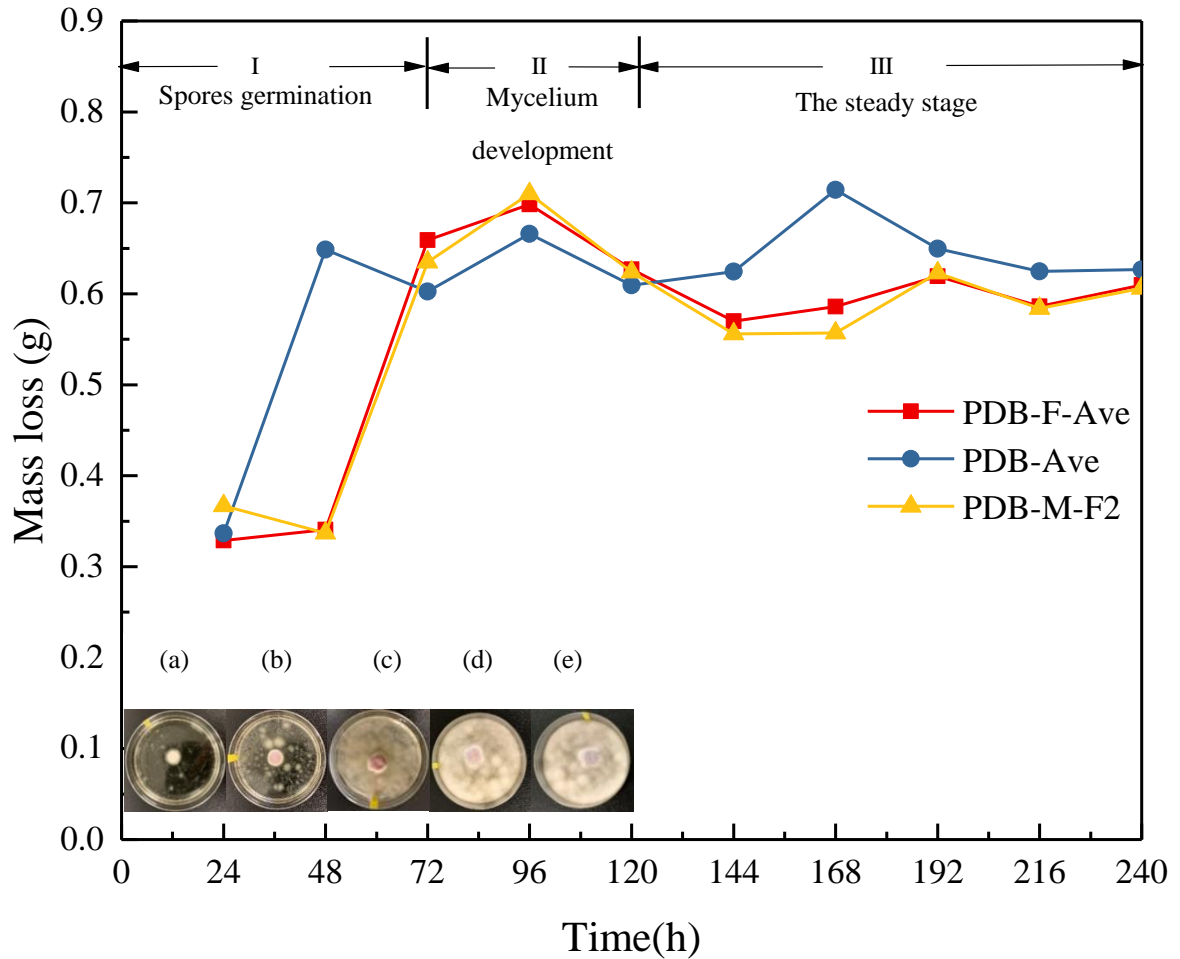
The mass change process of the growing system of samples including mortar, PDB and fungal mycelium, was complex and closely related to the evaporation and assimilation of fungal growth. It involved physical change, chemical reaction, and biological effects, which might couple with each other. For example, fungal assimilation contributes to mass loss and might also affect other physical changes. Complete capturing such factors are very difficult if not impossible. The mortar plates used for the testing were cut from mortar specimens cured for 90 days. To ensure the consistency in different samples, mortar slices were selected stochastically and avoided the selection of mortar slices from both ends of casted mortar specimens. The mortar plates were subjected to high temperature (in the oven with 100 °C for two hours) to sanitize prior to testing. It was placed into nutrient solution after treatment. Majority of hydration has taken place at that stage. Besides, the hydration reaction does not generate air that is released from the environment, and therefore the mass change is negligible in principle.

It is also noted that the testing was conducted in close cells with small ventilation holes and under a controlled temperature and humidity environment. It is assumed that the differences in mass loss such as evaporation due to the environment is insignificant.

For the reasons discussed, the mass change of mortar samples was attributed primarily to the metabolism of fungal growth. Therefore, the mass loss in each sample was measured to investigate the characteristics of fungal mycelium development and to summarize them into a typical growth pattern. Visual observations on the status of fungal growth were also captured to corroborate the observed trends of mass changes, with photos of the fungi growth taken at different stages.

The mass of each specimen was monitored over time. Figure 4 shows the monitored mass loss over 24 hours. These include the average values of observed 24-hr mass loss in PDB and PDB-F (PDB with inoculated fungi), and as well as 24-hr mass loss in PDB-M-F (cut mortar sample with PDB and inoculated fungi). The mass changes of mortar can be ignored in this system. Since these samples were placed under the same environment, the mass loss due to environmental evaporation should be similar. Therefore, the average mass loss in pure PDB serves as the baseline for comparison.



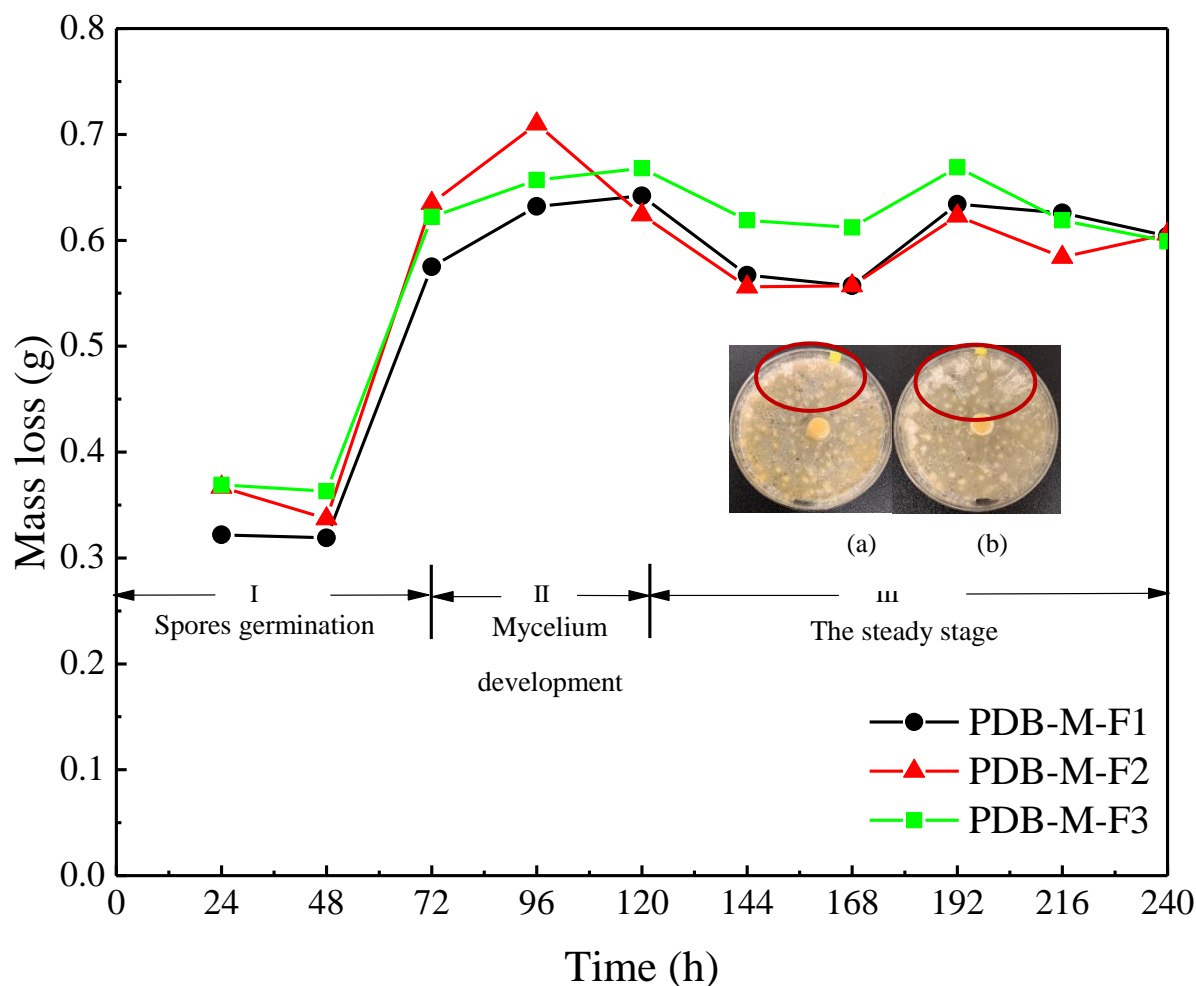


**Fig. 4** Mass loss in PDB and PDB-F group as well as PDB-M-F2 sample. The embedded images corresponding to the changes in PDB-F samples: (a) Several spores germinated at 24 hours; (b) Original inoculum grew and increasing spores sprout at 48 hours; (c) Mycelium cover the surface of Petri dish at 72 hours; (d), (e) Mycelium grew thicker and became stable at 96 and 120 hours.

Only physical change (evaporation) occurred in the PDB samples. The average evaporation rate was calculated as 0.65 g/day. In general, the growth of *Fusarium oxysporum* appeared to be in three stages.

- Stage I (0 h ~ 72 h): The germination of sparse spores. Several spores in different locations germinated in the first 24 hours. The mass loss in the groups of PDB (0.336g) and PDB-F (0.329g) in the early stage were similar; however, the mass of PDB-M-F2 sample was larger (by 0.03 g). It was conjectured that the introduction of mortar in the system, which showed a dark color compared with the color of PDB, resulted in an increased absorbance of light and higher temperature and evaporation rates. The mass change in the samples only containing PDB (0.648g) is almost two times that in the samples with *Fusarium oxysporum* (0.341g and 0.337 g) between 24 h and 48 h. Meanwhile, increasing spores germinate and the intimal inoculum grows. It indicates that the presence of *Fusarium oxysporum* results in less amount of water escaping via evaporation. After being inoculated, *Fusarium oxysporum* gathers and stores nutrition in the local environment to sprout.
- Stage II (72 h ~ 120 h): The vigorous development of mycelium. In the next 3 days, mycelium demonstrated significant radial extension and the numerous aerial hyphae developed vertically. The fungal colony become larger and denser in this stage. The assimilation associated with mycelium growth has a major impact on the system, as shown from the faster mass loss in the PDB-F group.
- Stage III (120 h later): The steady stage. The fungal growth has become stable, and mycelium has covered the surface of Petri dishes, which in turn reduced the evaporation in the system. Therefore, the mass loss in the PDB-F group is less than that of PDB group after 120 h due to the complete coverage of mycelium. In the samples with mycelium development (Group A and B), mortar has limited effects on the mass development of *Fusarium oxysporum* resulting from their similar mass loss trends.

Figure 5 summarizes the observed mass loss process of PDB-M-F2 (with mycelium development), PDB-M-F1, and PDB-M-F3 (both without obvious mycelium developments). The peak of daily mass loss appeared between 72h to 120h for PDB-M-F2, after which the rate of daily mass loss decreased. On the other hand, the greater mass loss appeared in PDB-M-F1 and PDB-M-F3 from 168 h, indicating fungal germination possibly also occurred in these two samples but with lower metabolism rates. Embedded photos show the visually observed fungal growth behaviors in PDB-M-F1 (a) at 168h, (b) 216h, which are to corroborate the experimentally observed mass loss behaviors.



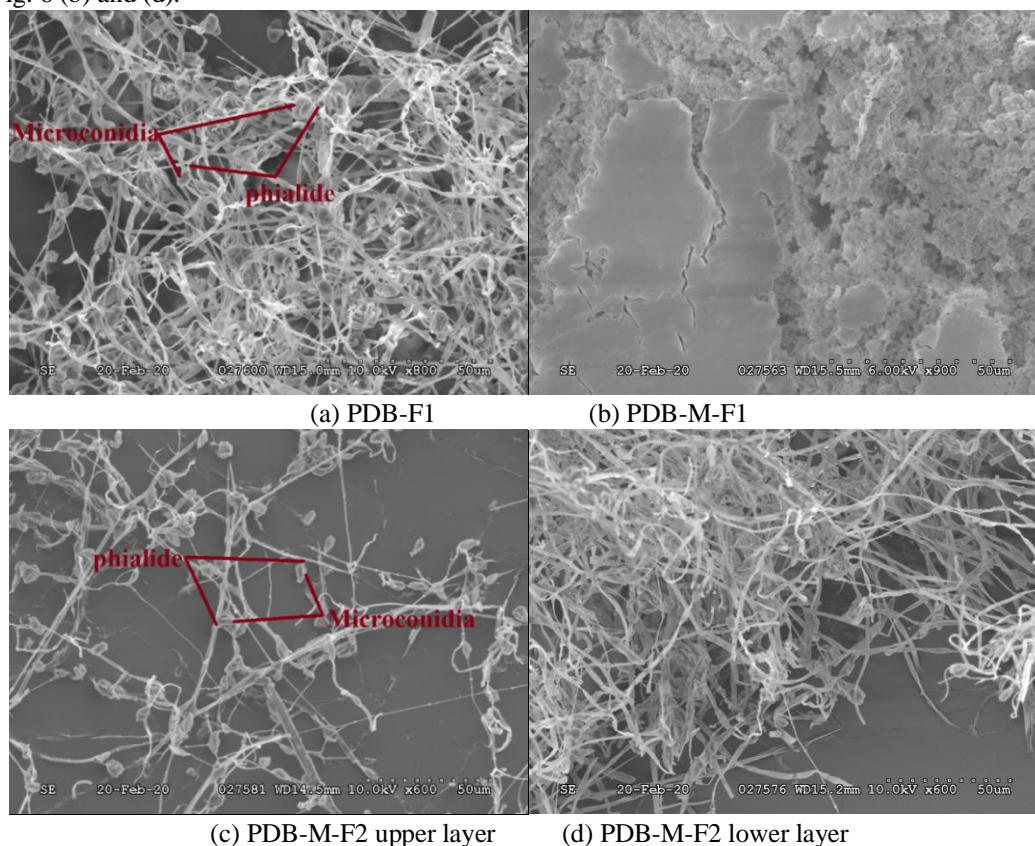
**Fig. 5** Monitored mass loss in PDB-M-F group. The embedded images corresponding to the changes in PDB-M-F1 sample: (a) Visually observed white hyphae germinated from the top edge at 168 hours; (b) Visually observed hyphae grew and developed from the edge to center at 216 hours.

#### Characteristics of microstructure and composition of healing components

*Fusarium oxysporum* is an asexual fungus. It has been confirmed that fungi feature tip growth, which can last for hundreds of years [9-11]. During the sprouting process, it produces aerial mycelium and the protoplasm migrates into the younger parts of the mycelium [12]. Microconidia (one or two-celled), macroconidia (three to five-celled), and chlamydospores (one or two-celled), are three types of spores produced by *Fusarium oxysporum* [13, 14].

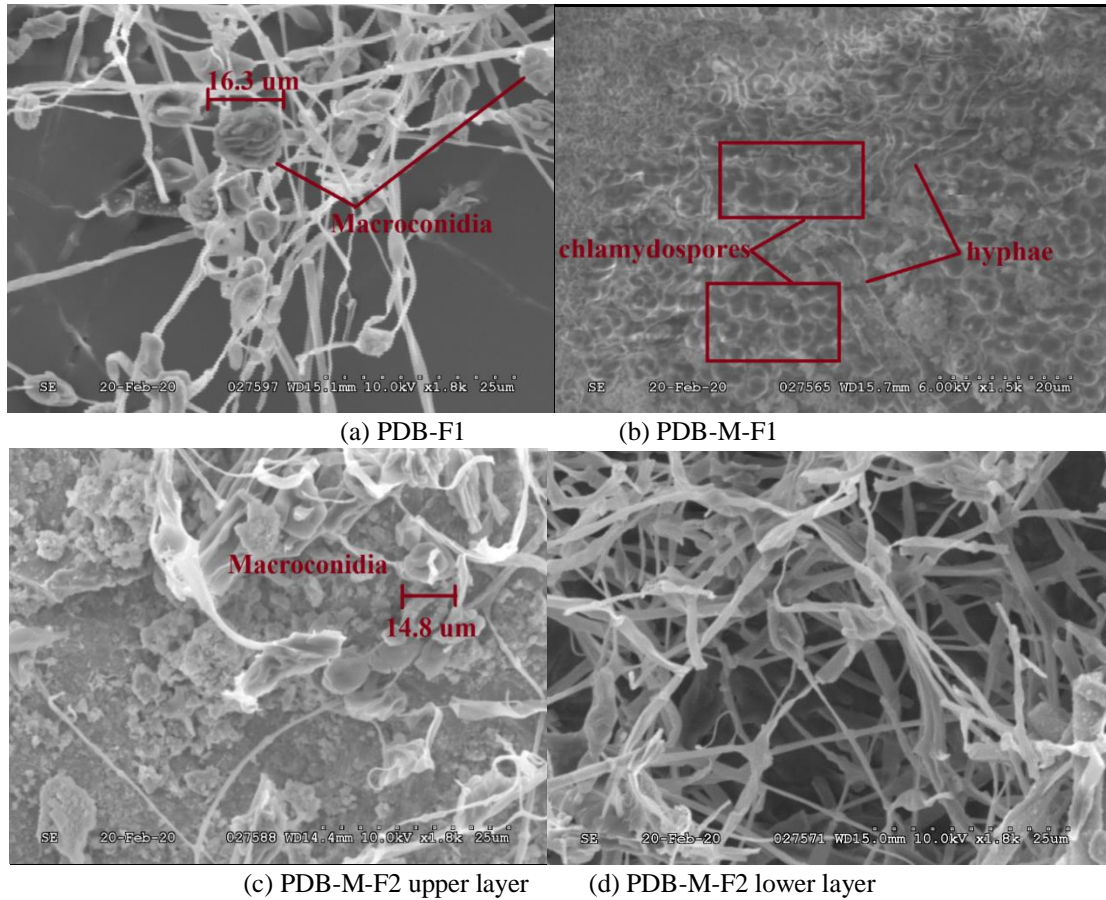
The four samples were collected from PDB-F1, PDB-M-F1, the upper layer of PDB-M-F2, and the lower layers of PDB-M-F2 were subjected to SEM in order to observe the characteristics of their microstructure. The representative SEM images were shown in Figure 6. The images were collected in high vacuum mode with a magnification of x600-x900. Numerous fungal hyphae were observed in Fig. 6 (a), (c) and (d) (corresponding to samples from PDB-F1, the upper layer of PDB-M-F2, and the lower layer of PDB-M-F2 respectively), while no obvious fungal hyphae were seen in Fig. 6(b) (from PDB-M-F1). Fungal spores were observed in Fig. 6 (a) and (c), as illustrated as microconidia spores that were born

on phialides arising laterally. They were oval-ellipsoid shaped with the size of around 5  $\mu\text{m}$ , and nonseptate. No spore was identified in Fig. 6 (b) and (d).



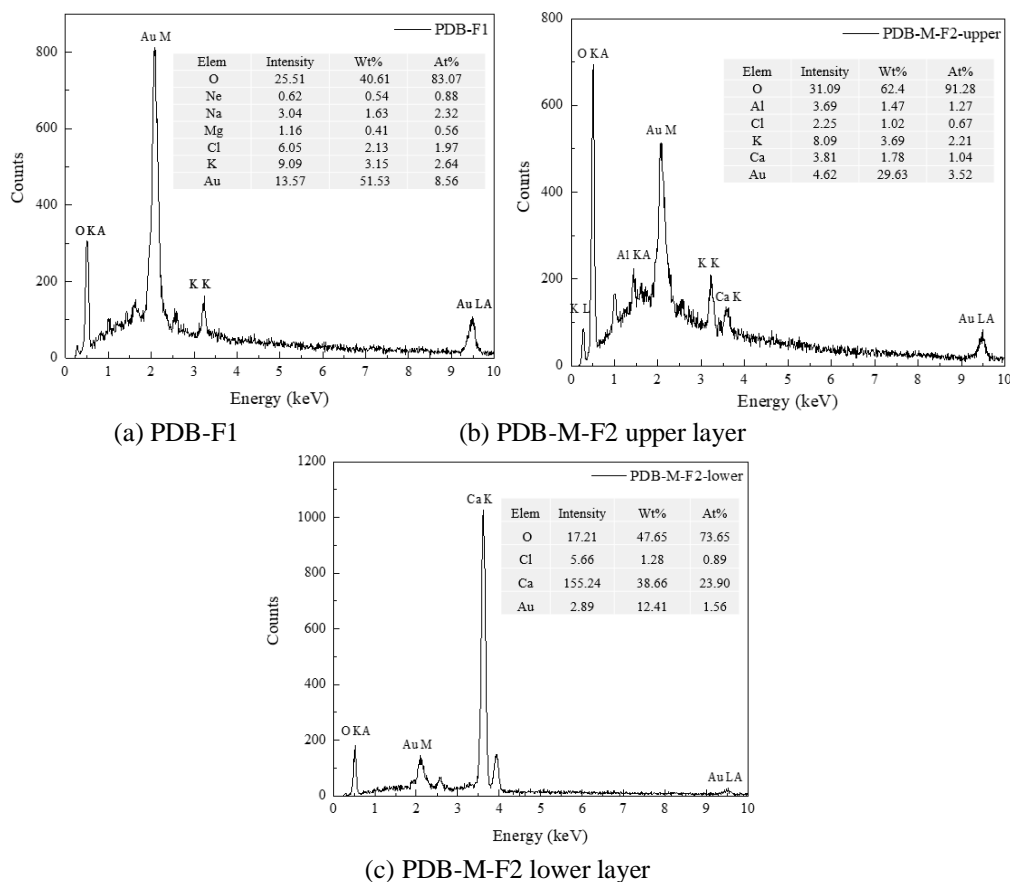
**Fig. 6** SEM image of morphology in (a) PDB-F1, (b) PDB-M-F1, (c) PDB-M-F2 upper layer and (d) PDB-M-F2 lower layer

Figure 7 shows the microstructure with a higher amplification factor (x1500 and x1800). Macroconidia, abundant and sparse, were found in Fig. 7 (a) and (c). Macroconidia spores are three- to five-septate and with a diameter of 15  $\mu\text{m}$ ; they are borne on branched conidiophores or the surface of sporodochia, fusoid-subulate and pointed at both ends, with a pedicellate base. Scattered distributions of hyphae were also seen in Fig. 7 (b). Spherical particles annotated in Fig. 7 (b) are chlamydospores which feature both smooth and rough walled, and being solitary generally but occasionally form pairs or chains [15]. Comparing (d) with (c) both in Fig. 7 and 8, only a few phialides with Microconidia and Macroconidia were discovered in the (d), which indicates the fungal hyphae in the lower layer retain limited regeneration activeness compared with that in the upper layer. The observation is consistent with the growth pattern by fungi, which has been reported to feature tip growth and last for hundreds of years [9-11]. The remarkable ability of fungi to produce the aerial mycelium to reach nutrition as well as the migration of protoplasm into the younger parts of the mycelium has been the subject of intense attention [12]. From the observed SEM image, most of the hyphae in the lower layer are the older ones, which are vacated and lose the ability to produce branches and spores. The fungal spores were enduring and could remain dormant in soil for as long as 20 years; they can also spread widely [16]. These characteristics can potentially ensure durable self-healing performance for concrete cracks.



**Fig. 7** SEM image with higher amplification factor in (a) PDB-F1, (b) PDB-M-F1, (c) PDB-M-F2 upper layer and (d) PDB-M-F2 lower layer

The EDS spectra were used to examine the chemical compositions on the surface of the samples that show obvious mycelium development (i.e., PDB-F sample and PDB-M-F2 samples). Three distinguished samples were analyzed. Two of them were from the upper layer and lower layer in the PDB-M-F2 sample respectively, while the other one was randomly selected from the PDB-F1 sample. The weight percentage (Wt.%) and the atomic percentage (At.%) of the compounds in these three samples were obtained and shown in Fig. 8. There are differences between samples obtained from the upper layer and the lower layer of PDB-M-F2. The EDS results show the calcium content in the mycelium fiber in the lower part (Wt%=38.66, At%=23.90, Fig. 8c) is much higher than that in the upper layer (Wt%=1.78, At%=1.04, Fig. 8b). This is consistent with the fact that the lower layer of the fungi mycelium closely interacts with the plain mortar surface and the upper layer grows into air. The higher concentration of calcium ions led to its higher likelihood to react with extracellular substances on the fungal cell walls' surface to produce calcium oxalate precipitation. The mortar-free samples (PDB-F) have limited access to calcium, limiting calcium absorption by the fungal mycelium. Consequently, no calcium is shown in the EDS spectrum of the PDB-F samples (Fig. 8a).

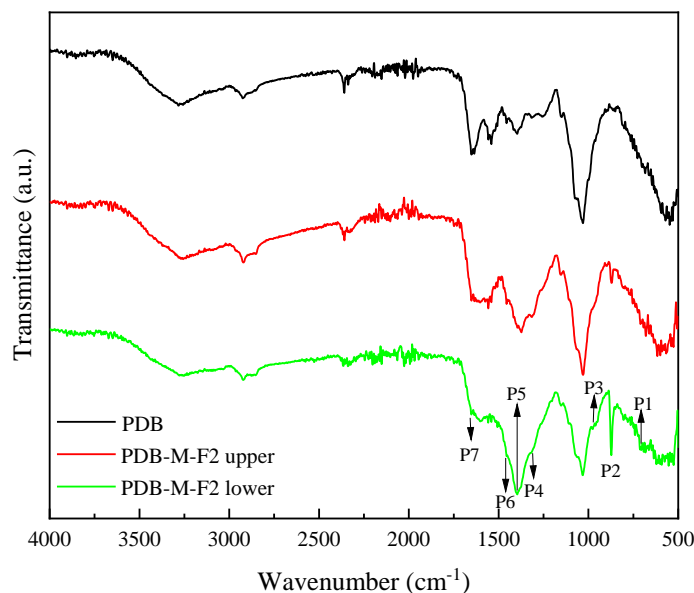


**Fig. 8** EDS spectra of samples collected from (a) PDB-F1, (b) PDB-M-F2 upper layer, and (c) PDB-M-F2 lower layer

### Chemical bond analyses with FTIR

Infrared (IR) spectroscopy (Fig. 9) illustrates the representative infrared spectra of fungal samples cultivated with pure nutrition (PDB-F1) or growing on the plain mortar surface (PDB-M-F2-upper, and PDB-M-F2-lower). The broad band at  $1430\text{ cm}^{-1}$ , the sharp band at  $876\text{ cm}^{-1}$ , and the weak band at  $712\text{ cm}^{-1}$  were observed due to the form of calcite in the 100 %  $\text{CaCO}_3$  [17]. The  $1437\text{ cm}^{-1}$  (P7),  $870\text{ cm}^{-1}$  (P2) and  $712\text{ cm}^{-1}$  (P1) bands appeared in different samples, which is close to the bands in pure  $\text{CaCO}_3$ . A few characteristic peaks in the FTIR were identified. P7 appears as a shoulder of the broad  $1397\text{ cm}^{-1}$  (P6) band, which is not as broad as described in previous study [17]. The in-situ formed  $\text{CaCO}_3$  in the samples and interacted with fungal substrate, causing the shift of bands. It provides evidence that fungal hyphae can bind calcium ions and produce  $\text{CaCO}_3$  precipitation. It is also concluded that the plain mortar supplied additional calcium for fungi, which increased the intensity of the bands (P1 and P2). Additionally, the appearance of bands at  $1316\text{ cm}^{-1}$  (P5) and  $1632\text{ cm}^{-1}$  (P8) in all these three samples validated the presence of calcium oxalate monohydrate. The strong bands at  $1632\text{ cm}^{-1}$  and  $1316\text{ cm}^{-1}$  are attributed to the asymmetric and symmetric vibrations of the oxalate group respectively. Another band at  $955\text{ cm}^{-1}$  (P3) is also corresponding to the existence of calcium oxalate monohydrate, explained by [18]. Fungi cultivated in a different environment keep the ability to produce oxalic acid [19], which contributes to the calcium oxalate. Additionally, the proteins and lipids bands, due to  $-\text{COO}-$  symmetric stretching, are centered at  $1397\text{ cm}^{-1}$  (P6) [20]. A4 reveals a combined area containing several bands' appearance, appearing at  $1085\text{ cm}^{-1}$  ( $-\text{PO}_2-$  in phospholipids) and at  $1050\text{ cm}^{-1}$  ( $-\text{C-O}-$  stretching of carbohydrates) [20]. The different inoculating environments possibly have changed the protein and lipids ratios in the fungal hyphal structure through the comparison of the intensity of P6 and A4 in different samples.





**Fig. 9** The FTIR results of fungi cultivated in different environments (note: P1 (712  $\text{cm}^{-1}$ ), P2 (870  $\text{cm}^{-1}$ ) and P7 (1430  $\text{cm}^{-1}$ ): calcite; P3 (955  $\text{cm}^{-1}$ ), P5 (1316  $\text{cm}^{-1}$ ) and P8 (1632  $\text{cm}^{-1}$ ): calcium oxalate monohydrate; P6 (1397  $\text{cm}^{-1}$ ): -COO- symmetric stretching; A4 (1085  $\text{cm}^{-1}$  and 1050  $\text{cm}^{-1}$ ): -PO<sub>2</sub>- in phospholipids and -C-O- stretching of carbohydrates)

#### Contact angle measurement

To clarify the surface property of fungal mycelium, the contact angle test was performed. Fungal mycelium samples were collected from the fungi growing with pure nutrition (PDB-F group) and growing with nutrition and mortar (PDB-M-F group). Each step of the experiment was performed carefully to ensure the mycelium film was not contaminated. The fungal inoculum was initially inoculated to the sterile Petri dishes. The Petri dishes were covered by lids during the growing process. Fungal hyphae grow in the air, which are called aerial hyphae, and they are covered by hydrophobic protein. Its hydrophobicity had a self-cleaning effect and made the top surface of mycelium clean. The testing mycelium was transferred to a new and sterile Petri dish with a cover prior to the contact angle test. All of the operations, including adding nutrition and transferring mycelium, were fulfilled in a laminar flow hood, which provided a clean environment. These ensured that the samples used for contact angle measurements were not contaminated by other factors.

The measured contact angles on both sides of the water-mycelium interface are summarized in Table 4 and Table 5. The average contact angles of fungal mycelium film in groups of PDB-F and PDB-M-F were 131.47° and 134.92°. The *Fusarium oxysporum* mycelium fibers cultivated with plain mortar showed higher contact angles, which indicates stronger water repellent. The hydrophobicity of *Fusarium oxysporum* mycelium, when covering the surface of concrete or mortar, will potentially help reduce water infiltration into cement mortar.

**Table 4** Contact angle (CA) of fungal mycelium film in PDB-M-F group

No.	CA left (°)	CA right (°)
1	132.7	133.0
2	131.0	131.0
3	140.1	140.5
4	136.6	137.1
5	133.5	133.7
<b>Mean ± SD</b>	<b>134.78 ± 3.22</b>	<b>135.06 ± 3.36</b>

**Table 5** Contact angle (CA) of fungal mycelium film in PDB-F group

No.	CA left (°)	CA right (°)
1	137.4	137.6
2	128.9	127.9
3	136.2	136.6
4	127.3	128.2
5	127.6	127.0
<b>Mean ± SD</b>	<b>131.48 ± 4.39</b>	<b>131.46 4.63</b>

### 2.1.3 Summary of Experimental Observations and Performance Prediction

#### *The feasibility of healing concrete crack with *Fusarium oxysporum**

The experimental observations demonstrate the growth behaviors of *Fusarium oxysporum* on the surface of mortar. While high pH pore environment appeared to inhibit the growth of mycelium, the fungal mycelium is still able to grow quickly to cover large area and develop spores for sustained growth. The mycelium is able to assimilate nutrition and produce calcium mineral, a self-healing agent. Besides, the high hydrophobicity of mycelium presents unique opportunities to mitigate infiltration of corrosive fluid into concrete matrix. The feasibility of fungi for crack healing is analyzed based on the unique characteristics of fungi.

#### *Growth rate of *Fusarium oxysporum* cultivated at different pH*

As shown in Fig. 2, fungal samples in Group A and B demonstrate different mature time, which is defined as the time to completely cover the surface of the mortar sample. The mature time in Group B is 72 h, while it is 96 h in Group C due to slightly higher pH. For both cases, the sprouting time occurred in about 0.33 of the mature life. A normalized plot of Fig. 2 is developed and shown in Fig. 10, where the horizontal axis is divided by the time with mature time and the vertical axis is divided by the increasing surface with the initial area of inoculum. Fig. 10 shows that the fungal samples in different groups had similar growth behaviors. While high pH decelerated the growth rate of fungal mycelium, it had little influence on their growth pattern. From this observation, the mature time was predicted by the spore germination time (168 h) observed in the Group C, which led to a mature time of 504h. That is, the mature life of fungal mycelium in Group C has been extended to 8 times of that in Group A due to the high alkaline environment.

The fungal mycelium growth behaviors found can be described with an exponential equation (Equation 1). The empirical model defines where fungal mycelium develops at an initial rate  $g_0$ , and then increases exponentially with time  $t$ , until its mature stage. The growth rate (defined as the area covered by the fungi to the area of initial fungi inoculum) is shown in Equation 1:

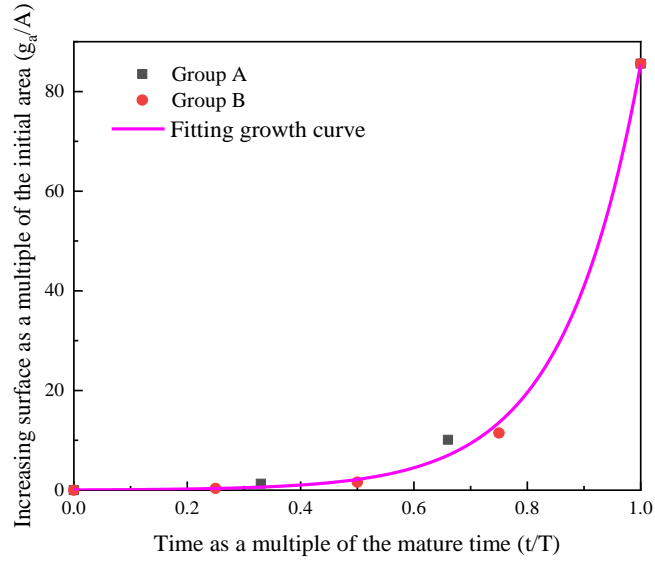
$$g_a = g_0 e^{k(\frac{t}{T})} \quad (\text{Eq. 1})$$

where  $g_a$  is the growth rate at time  $t$ ;  $g_0$  is the initial growth rate;  $T$  is defined as the mature time which is the observed time for fungi to completely cover the surface of mortar specimens and is primarily used to normalize the actual time  $t$ ,  $k$  is the rate constant that determines the growth speed.

The best-fit coefficients for this equation based on experimental data are  $g_0 = 0.0543$ , and  $k = 7.362$ . Thus, Eq. 1 can be written as:

$$g_a = 0.0543 \times e^{7.362(\frac{t}{T})} \quad (\text{Eq. 2})$$

The Adj. R-square for the fitting equation is 0.997.



**Fig. 10** Growth curve of Group A and B after normalization

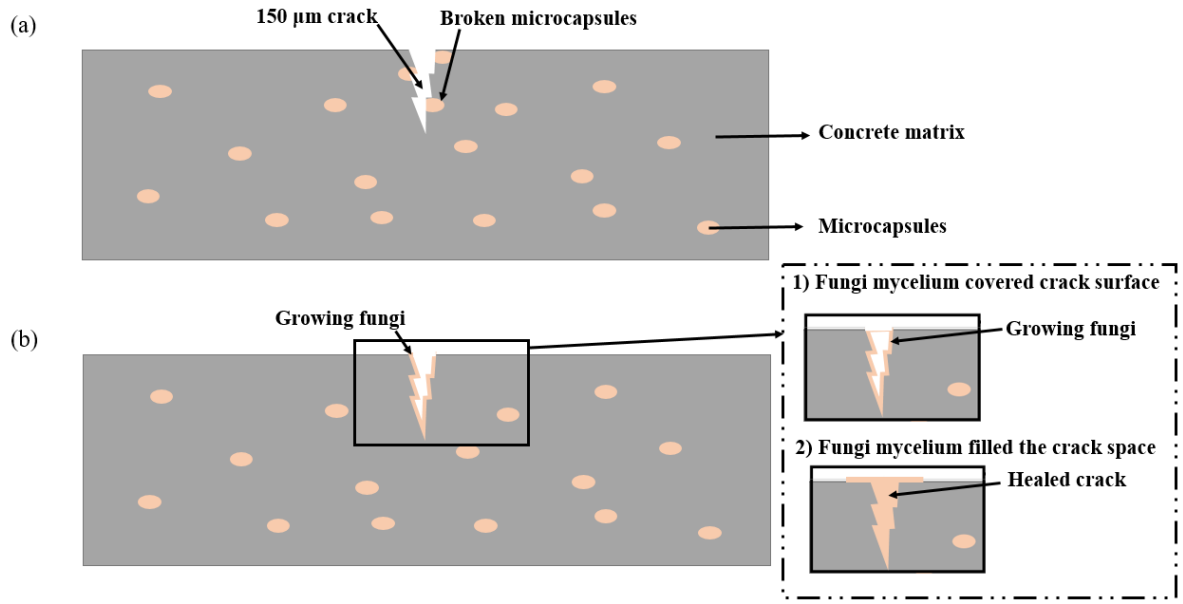
#### ***Performance of *Fusarium oxysporum* in healing concrete cracks***

The feasibility of using encapsulated *Fusarium oxysporum* fungi to heal concrete cracks is analyzed conceptually (Fig. 11). It was observed that for a prism of 30 mm × 30 mm × 360 mm that contained 5% by weight of microcapsules containing healing agent, a crack of 150 μm width was healed by bacteria based healing agents in about 3 weeks as reported by [21].

For a comparison, the self-healing performance with 5% microcapsules by volume that contain fungal spores and nutrition medium is analyzed. Assuming the microcapsules of 10 μm radius with fungi-mediated healing agent is uniformly embedded into concrete mix, for a concrete prism of 30 mm × 30 mm × 360 mm, the overall area of microcapsules on one surface is 540 mm<sup>2</sup> (or 5% of the surface area). For a crack of 150 μm in width and 1mm in depth across a concrete surface, the total volume of the crack is 4.5 mm<sup>3</sup>, 5% of this volume would include about 71619 micro-encapsulates of radius 10 μm. It is assumed that the fungal spores will have high chance to start to germinate when the capsules in the crack area are broken by crack generation.

It is calculated that the mature time in 150 μm crack is 0.796 T (T is mature time of fungal mycelium development). The time for healing the cracks at different levels of pH has been summarized in Table 6. Compared with bacteria-based healing, the fungal encapsulated self-healing technique potentially decreases the healing time to 11.3%, 15.1% and 79.6% at different pH levels and thus improve healing efficiency.





**Fig. 11.** Schematic illustration of the mechanism of self-healing concrete with encapsulated fungal spores (a) Concrete cracks breaks microcapsules and releases fungi (b) Fungi cover the crack surfaces (short term) and heal the crack (long term)

**Table 6** The healing time by *Fusarium oxysporum* at different pH

pH levels	Healing time	Percentage of time by bacteria induced healing (3 weeks or 21 days) <sup>2</sup>
Group A <sup>1</sup> (<9)	2.38 day	11.3%
Group B <sup>1</sup> (~9)	3.18 day	15.1%
Group C <sup>1</sup> (>12)	16.71day	79.6%

<sup>1</sup> The healing condition (pH) is similar to sample in Group A, B and C.

<sup>2</sup> Wang, Soens et al. 2014

#### Assessment of reduction of liquid infiltration into concrete

Cracks in concrete accelerate water infiltration to the concrete matrix, which leads to accelerated deterioration by corrosion, freeze-thaw cycles, etc. Corrosion of steel rebar typically occurs when water containing corrosive salt reaches the reinforcement. Additionally, large internal force can be produced in concrete structure when water in the concrete pore space is subjected to the freeze-thaw cycles. Treatment with hydrophobic surface coating has been used to repel water from infiltration into concrete [22, 23]. The hydrophobicity of fungi mycelium forms a hydrophobic coating that fills the crack surfaces and forms a water-repellent barrier, which helps to limit the rate of water infiltration and absorption into concrete. Fungi are generally believed to contribute to the water repellency observed in an agricultural soil [24, 25]. The equation 3 is widely used to describe the relationship between the contact angle and the infiltration rate into a porous medium [26].

$$f_q = \frac{Cr^2\rho gh}{8L\eta} + \frac{2Cr\gamma\cos\theta}{8L\eta} \quad (\text{Eq. 3})$$

where  $f_q$  is the infiltration rate, i.e., the infiltration volume per unit surface and per unit time;  $C$  is the water content (volume fraction) of the porous medium;  $r$  is the effective pore radius;  $\rho$  is the liquid density;  $g$  is the gravitation constant;  $h$  is distance from the water surface to the wetting front;  $L$  is the distance from the soil surface to the wetting front;  $\eta$  is the liquid viscosity;  $\gamma$  is the liquid surface tension and  $\theta$  is the contact angle.

The first term on the right-hand side of Equation 3 describes the infiltration driven by gravity; while the second term describes the infiltration due to surface energy such as capillary, which is affected by the liquid solid surface contact angle. The infiltration rate due to gravity potential is not affected by the surface characteristics of concrete, i.e., water repellency. Therefore, the differences in the water infiltration rates is primarily due to the differences in the surface energy, described by the contact angle.

Using the measured contact angle of the regular concrete, which is around 40° [22], and the average contact angle of 134.92° for the concrete covered with fungal mycelium, the calculated infiltration rates are 0.453 g/(m<sup>2</sup>·s) and 0.078 g/(m<sup>2</sup>·s) through regular concrete surface versus concrete surface covered with fungi respectively. The parameters applied to calculate the infiltration rate are listed in Table 7. This implies that when the surface of concrete cracks is covered with fungi as part of the healing process, the infiltration rate is reduced to 17.22 % of that through regular concrete surface theoretically.

**Table 1** Parameters applied in the infiltration rate calculation using Equation 3

Parameter	Unit	Regular concrete	Reference	Fungi mediated concrete
$C$		0.03	[27]	0.03
$r^I$	m	2.5e-6	[28]	2.5e-6
$\rho$	Kg/m <sup>3</sup>	1000		1000
$g$	m/s <sup>2</sup>	9.8		9.8
$\gamma$	N/m	7.28e-6		7.28e-6
$\eta$	Pa·s	8.90e-4		8.90e-4
$h/L^2$	m	6.03e-4	[22]	6.03e-4
$\theta$	°	40	[22]	134.92
$f_q$	g/(m <sup>2</sup> ·s)	0.453	[22]	0.078

<sup>1</sup> The capillary pore size given in [28] is 10 nm ~10000 nm, thus the average pore radius was used to describe the effective pore radius.

<sup>2</sup> Calculated by the infiltration rate in regular concrete.

### 2.1.3 Summary of Phase 1 Investigation

Activities in this stage explored the potential of filamentous fungi, *Fusarium oxysporum*, as a microbial agent to heal concrete cracks, due to its capability to precipitate calcium-based minerals, to reinforce concrete matrix with fungal hyphae, and to impede water infiltration with hydrophobic surface. Contrast experiments were conducted to observe the characteristics of the fungal mycelium development behaviors on the surface of mortar. The results showed that *Fusarium oxysporum* was able to germinate on the surface of mortar and showed rapid growth behaviors in covering the surface with mycelium fibers. However, the mycelium development was influenced by the pH value, with high pH delays the germination time and increased the mature time (defined in this paper as the time that mycelium completely covers the surface of mortar). The growth behaviors of *Fusarium oxysporum* all included three stages, i.e., the germination of spores, the development of mycelium, and the steady growth. Under favorable conditions, *Fusarium oxysporum* mycelium covered a surface area of mortar 86 times the area of the original fungi inoculum after 96 hours. Such fast growth of *Fusarium oxysporum* could contribute to high efficiency in healing cracks.

The microscopic characteristics of fungi mycelium were analyzed with advanced instrument such as SEM/EDS, and FTIR. The SEM images confirmed that *Fusarium oxysporum* was able to germinate spores and develop mycelium despite

of the high pH value on mortar surface. Fungal mycelium is able to precipitate calcium minerals by using the calcium source in mortar pore fluid, which would contribute to healing cracks. The FTIR spectra confirmed the presence of calcium carbonate and calcium oxalate monohydrate, which are the resultants of the metabolism by fungi.

The fungal mycelium is hydrophobic with an average contact angle of  $134.92^\circ$  when grown on the surface of mortar, which is slightly larger than  $131.47^\circ$  contact angle observed in the regular mycelium. Such larger contact angle when concrete surface is covered with fungi mycelium would lead to higher water repellency and consequently would help reduce water infiltration into concrete through the cracks.

Based on the experimental observations, feasibility analyses were conducted to demonstrate the potentials of *Fusarium oxysporum* to improve concrete durability by rapidly covering and healing concrete cracks and mitigating water infiltration. The unique characteristics of fungi (i.e., its ability to survive pore environment in concrete, its rapid growth, its ability to precipitate calcium minerals, and its water repellency) makes it a compelling candidate for self-healing concrete. Compared with bacteria based self-healing concrete, fungi can potentially significantly increase the healing efficiency (only requires 11.3%, 15.1% and 79.6% of the healing time by bacteria mediated MICP depending upon the pH levels). Besides, the water repellency of mycelium would reduce the water infiltration rate to 17.22% of that of the regular concrete surface, which is another advantage over bacteria induced MICP in improve the durability of concrete. In addition, fungi provide an environmentally friendly way to heal concrete cracks, since no toxic gases are released to the atmosphere as in MICP process. Overall, in Stage 1, *Fusarium oxysporum* was demonstrated as promising to be used to mediate self-healing of concrete cracks. This set the foundation for the further investigation in Phase 2.

## **2.2 Phase 2: Development of Scalable Production for Microcapsules Containing Fungi-Healing Agents**

### **2.2.1 Overview of the research goal**

Highly alkaline concrete is an adverse environment, which slows the activity of microorganisms, both fungi and bacteria, and undermines the efficiency of healing cracks [29]. Encapsulating technologies based on different protective materials such as calcium alginate, melamine-based materials, and polyurethane, have been developed to address such a problem. Among them, calcium alginate-based technology is the simplest and most effective method used in microbial-aided self-healing concrete [30]. In this method, calcium ions react with  $\alpha$ -L-guluronic acid (G residue) in alginate and produce a crosslinking structure, encapsulating bacterial spores [31]. The use of calcium alginate capsules containing spores led to a 39.6% increase in the flexural strength of cement mortars [32]. Wang et al [21] applied a melamine-based microcapsulation technique to carry bacterial spores, using inert substance to protect them. Wang's study indicates that compared to samples without bacteria, incorporating melamine-based capsules that contain bacterial spores enhanced the healing ratio by 30% and increased the maximum width of healable cracks fourfold [21]. Polyurethane (PU) has a large proportion of pores, making it a candidate for immobilizing bacterial cells, capable of keeping microbes enzymatically active for a prolonged period [29]. However, as an organic material, PU is incompatible with the concrete matrix [33].

These studies and others have promoted the adaptivity of bacteria in concrete, but other microorganisms should be considered. Fungi offers additional advantages when used for self-healing technique. To incorporate it into concrete effectively, investigating method of encapsulating fungi is necessary. Previous studies demonstrate that, like in bacteria-based self-healing concrete, the high pH in concrete significantly impacts the development of fungal mycelium [34]. Therefore, encapsulating technology is needed to ensure fungal growth in a harsh environment, such as when introducing them into concrete to heal cracks. Such encapsulation technology is crucial for promoting fungal metabolism activities in concrete and for enhancing the healing efficiency of fungi-based self-healing technique.

Based on the aforementioned motivation, Phase 2 investigates a biocompatible and effective method of encapsulating fungal cells in calcium alginate. This study demonstrates the workability of mortar mixture containing different amounts of capsules: 2%, 3.5%, and 5% weight ratio. Additionally, the healing rates of cracked samples containing these amounts of fungi-based capsules are studied as an indicator of fungi-based self-healing efficiency. Simultaneously, the impact of crack width on the performance of fungi-based self-healing technique is investigated. In addition, this study has elucidated the encapsulated fungi-based self-healing mechanism, which may provide valuable insights for the future development and implementation of fungi-based self-healing concrete. The findings in this stage also potentially lead to the refinement of encapsulated fungi-based self-healing technology and its wider application in the construction industry.

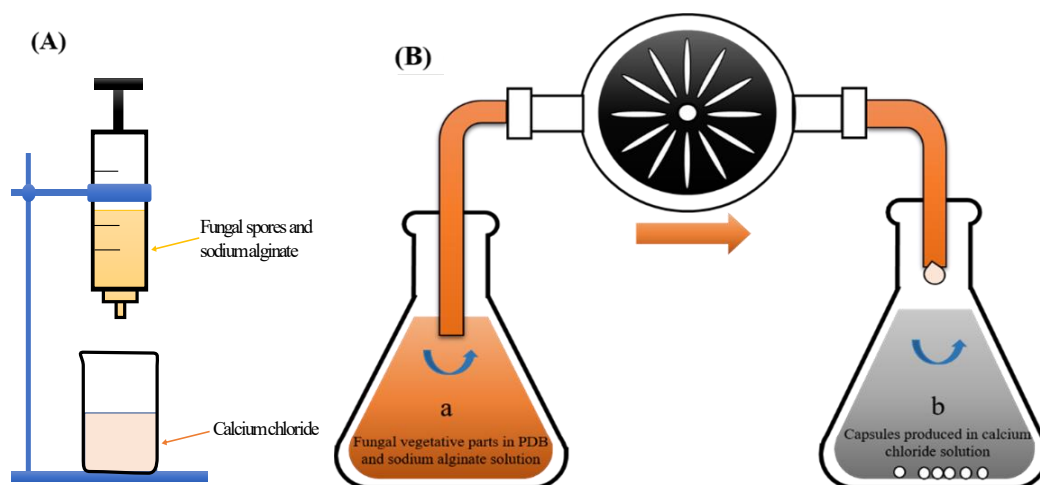
## 2.2.2 Experimental investigations

### Fungal strain and nutrients

*Fusarium oxysporum* (ATCC MYA-1198) forms filamentous structures that include branching, which grow in three dimensions. This filamentous structure is known as hyphae and allows for reproduction through spores or conidia [35]. Potato Dextrose Broth (PDB) (DF0549-17-9), a product of Fisher Scientific, was used for the cultivation of the fungal strain. A PDB solution with a concentration of 24 g/L was chosen as the nutrient source to support the growth of *Fusarium oxysporum*. Both the nutrient solution and containers were autoclaved at 120 °C for 15 minutes prior to the experiment.

### Comparison of two encapsulated systems

Two main chemical solutions were used to generate capsules containing fungi. Sodium alginate (18-606-287), which has been used in the food and pharmaceutical industries, was provided by Fisher Scientific. Calcium chloride (AC192735000) was also obtained from Fisher Scientific. Five fungal inoculums with a diameter of 5.75 mm were obtained from the leading edge of the original fungal colony and cultivated with 450 mL of PDB solution at 20 °C  $\pm$  2 °C and a relative humidity of 35%  $\pm$  3% for 5 days. The harvested PDB solution containing the fungal cells of *Fusarium oxysporum* was suspended in 450 mL of 2% (w/v) sodium alginate solution to obtain a homogeneous suspension. The suspension was extruded to calcium chloride solution by two systems. The first one is syringe-based encapsulated system, which extrudes the suspension into calcium chloride solution with a constant rate of 0.8 mL/min (Fig. 12A). The second one is pump-based encapsulated system. In this system, the suspension was compressed by a peristaltic pump with a constant speed of 18 mL/min to extrude free-fall droplets into 2% (w/v) calcium chloride solution. The droplets were left in the stirring calcium chloride solution for 30 minutes (Fig. 12B). The consequent reaction between sodium alginate and calcium chloride forms the capsules. These capsules were washed with sterile deionized water, dried at room temperature for 72 hours until completely dry. The diameter and density of the dry capsules are 1.4 mm and  $3.75 \times 10^{-4}$  g/mm<sup>3</sup>, respectively.



**Fig.12.** (A) Syringe-based encapsulated system; (B) Pump-based encapsulated system. Flask a: fungal cells in the solution of PDB and sodium alginate; flask b: capsules produced in the solution of calcium chloride.

### Sensitivity Study on the Amount of Nutrient in Microcapsules

Due to the comparatively slow extrusion speed inherent to syringe-based encapsulated systems, the pump-based encapsulated system was adopted for this project. The objective of determining the optimal nutrient quantity within the capsules was pursued, aiming to sustain fungal growth without necessitating additional nutrient replenishment. Such an achievement holds the potential to simultaneously streamline labor efforts and mitigate costs. This critical stage not only paves the way for the feasible implementation of fungi-based self-healing methodologies in practical settings but also underscores their viability for real-world applications.

#### Trial 1:


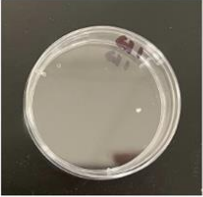
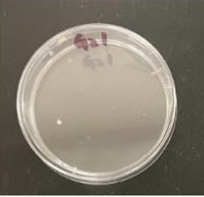
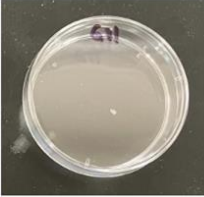

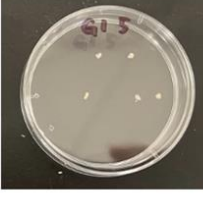
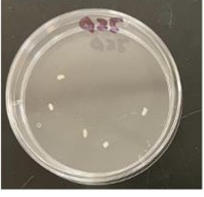
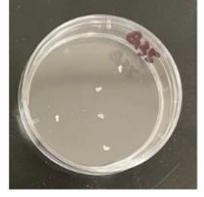

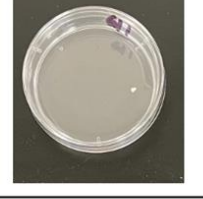
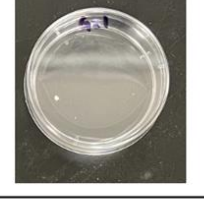
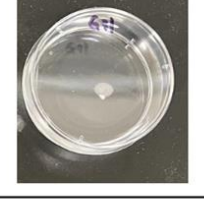

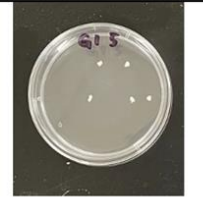
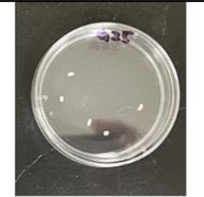
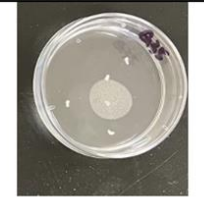
### Experiment:

The experiment consists of growing fungi for five days and harvesting the solution containing fungal cells, adding additional nutrients (PDB powders) during the fabrication of capsules at concentrations of 30 g/L, 45 g/L, and 60 g/L, and placing the wet capsules in a room with controlled temperature and humidity for three days to obtain dry capsules with an average diameter of 1.2 mm. To investigate the grouping effects on the growth of encapsulated fungi, an experiment was conducted in which different numbers of dry capsules were cultivated in both tap water and deionized water. The capsules were divided into two groups: a clustered capsule group and a single capsule group. Each group was placed in separate containers with the respective water type and incubated at controlled conditions for a period of time.

### Results:

Contrary to the initial hypothesis, the experimental results showed that fungi were unable to grow when cultivated in both tap water and deionized water. Despite providing adequate nutrient supply and controlled incubation conditions, the fungal cells in the capsules did not exhibit any signs of growth or germination. This unexpected outcome suggests that further investigations into the growth of encapsulated fungi without external nutrient supply are necessary. Moreover, alternative strategies for providing a suitable nutrient source may be required for the successful application of fungi-based self-healing technologies in concrete.

**Table 8** Results of Trial 1

Day	Number of capsules	G1_low	G1	G2	G3
1	1				
		G1_low	G1	G2	G3
1	5				
		G1_low	G1	G2	G3
7	1				
		G1_low	G1	G2	G3
7	5				

### *Conclusion:*

The main reasons why encapsulated fungi cannot grow in water are:

1. The size of the capsules is smaller than what generated in a previous study, with a diameter of 1.4 mm. Larger capsules incorporate more internal nutrients, providing a benefit for introducing large capsules in the concrete mixture. Additionally, larger capsules have a thicker wall that could offer strong protection for fungal growth in alkaline concrete.
2. The concentration of fungal cells in the solution may affect the growth or germination of fungi in water. There are controversial hypotheses regarding the influence of fungal cell concentration on fungal growth. One hypothesis suggests that a higher concentration of fungal cells provides more active spots for germination. While another suggests that a higher concentration of fungal cells will consume more nutrients. Under conditions of limited nutrients, the concentration of fungal cells should be lowered in single capsules.

### **Trial 2:**

Based on the outcomes of Trial 1, the focus was on increasing the size of capsules and investigating the effects of different concentrations of fungal cells. To achieve this, some adjustments were made during the generation of capsules and the experimental plan. The following adjustments were made:

1. The fungus was grown in a solution for varying periods to obtain different concentrations of fungal cells, referred to as fungal solution in the following text.
2. Additional PDB was added to the mixture of sodium alginate and fungal solution, resulting in an increase in the internal nutrient content of a single capsule.
3. The generated capsules were left in a calcium solution for at least 30 minutes to ensure sufficient time for encapsulation reaction.
4. Capsules cultured by DI water were compared with those cultured by varying concentrations of PDB.

### *Experiment:*

Two concentrations of fungal solution-with different growing time (C1< C2)

Two concentrations of PDB incorporated in capsules (24 g/L and 48 g/L; Cin)

Three concentrations of PDB in the cultivation solution (0 g/L, 24 g/L and 48 g/L; Cout)

Three different amounts of capsules (1, 3, 10)

### *Results:*











1. The concentration of both internal and external nutrients plays a significant role in the germination of encapsulated fungi. Regarding the effects of internal nutrient, fungi expand more with the increase of internal nutrient when comparing the fungal growth in sample C1-Cin24-Cout0 and C1-Cin48-Cout0. This conclusion also applies to external nutrient, where encapsulated fungi grow faster in C1-Cin24-Cout24 as compared to C1-Cin24-Cout0. Additionally, the encapsulated fungi exhibit purple color when grown in DI water and display white mycelium when cultivated in PDB solution.
2. With regards to the different concentrations of fungal solution and their cultivation in PDB solution, there was no significant difference in fungal growth during the early stages of sample C1-Cin24-Cout24 and C2-Cin24-Cout24. However, from Day 7 onwards, a faster growth rate was observed in the sample with a higher concentration of fungal solution (C2-Cin24-Cout24). When the samples were cultivated in DI water (without external nutrient supply), there was no visible difference in fungal growth between sample C1-Cin24-Cout0 and C2-Cin24-Cout0.
3. Comparing the fungal growth in C1-Cin24-Cout24, C1-Cin48-Cout24, and C2-Cin24-Cout24, it can be observed that internal nutrient plays a more significant role than fungal solution concentration, as faster fungal growth was observed in C1-Cin48-Cout24 than in C2-Cin24-Cout24.
4. Among the three different nutrient conditions tested - C1-Cin24-Cout24, C1-Cin48-Cout24, and C1-Cin24-Cout48 - the results indicate that internal nutrient availability exerts a stronger influence on fungal growth than










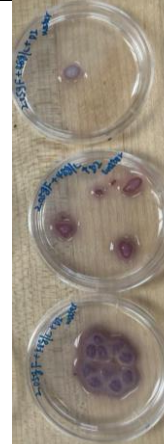







external nutrient supply. This is supported by the observation of faster growth in C1-Cin48-Cout24 as compared to C1-Cin24-Cout48.


5. In the situation with limited external nutrient, such as C1-Cin48-Cout24 and C2-Cin48-Cout24, increasing fungal solution doesn't work well. Increasing external nutrient is more effective for a cluster of capsules, as 10 capsules grow a larger mycelium in C1-Cin48-Cout48 then in C1-Cin48-Cout24 and C2-Cin48-Cout24.

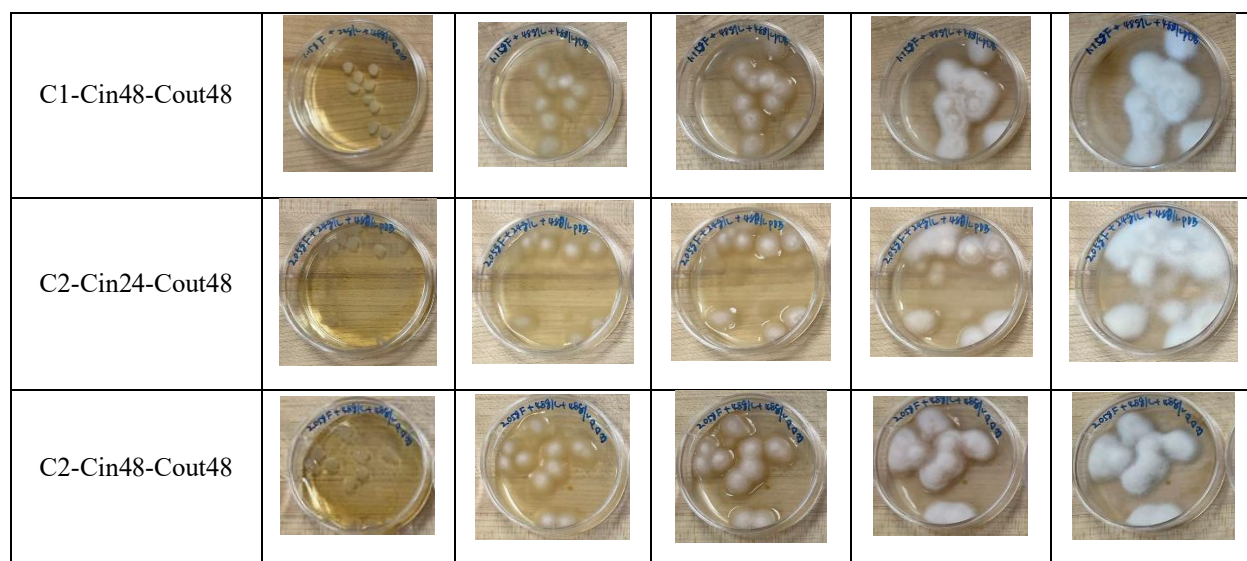
**Table 9** Results of Trial 2

Sample	Day 1	Day 3	Day 7	Day 15	Day 21
C1-Cin24-Cout0					
C1-Cin48-Cout0					

C2-Cin24-Cout0					
C2-Cin48-Cout0					
C1-Cin24-Cout24					



C1-Cin48-Cout24					
C2-Cin24-Cout24					
C2-Cin48-Cout24					
C1-Cin24-Cout48					



#### *Conclusion:*

1. Based on the result 3 and 4, it can be concluded that increasing the availability of internal nutrient within the capsule is crucial for promoting fungal growth and enabling practical application of encapsulated fungi-based self-healing techniques in scenarios with limited external nutrient supply.
2. When grown in DI water, which is an unfavorable environment for fungal growth, the fungal mycelium turns purple.

#### **Trial 3:**

##### *Experiment:*

Based on Trial 2's conclusion, the internal nutrient level was increased within a single capsule by adding 88.5 g/L, 100 g/L, and 120 g/L PDB during the fabrication process. The growth of capsules in these three groups was compared to that of capsules without any internal nutrient. The diameter of the generated capsules in the wet state is approximately 6 mm.

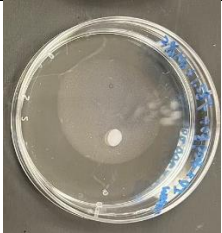

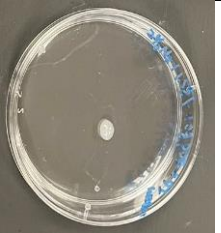
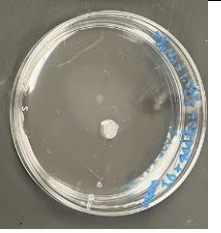
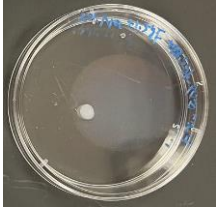
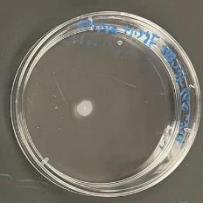
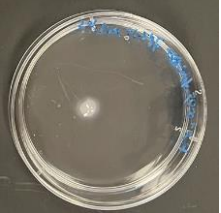
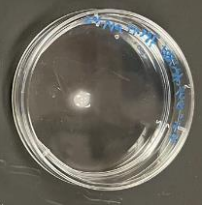


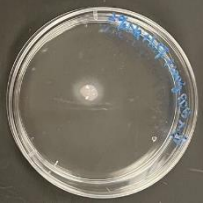
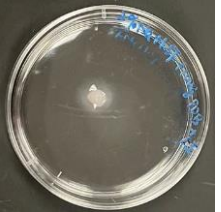
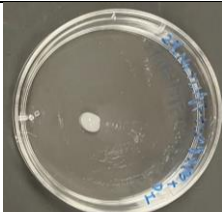

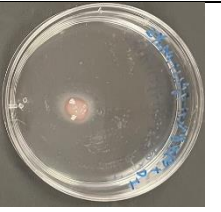
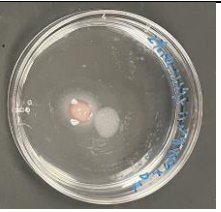

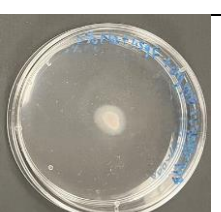
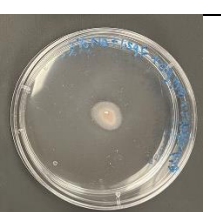

The concentration of external nutrients utilized in this study was 1.36 g/L. The choice to deviate from the typical concentrations of 24 g/L and 48 g/L, as used in Trial 2, was made with the objective of maintaining the total amount of nutrients within the growing system, including both external and internal sources. Thus, the total amount of nutrients in C2-Cin120-Cout0 and C2-Cin0-Cout1.36 are equivalent.

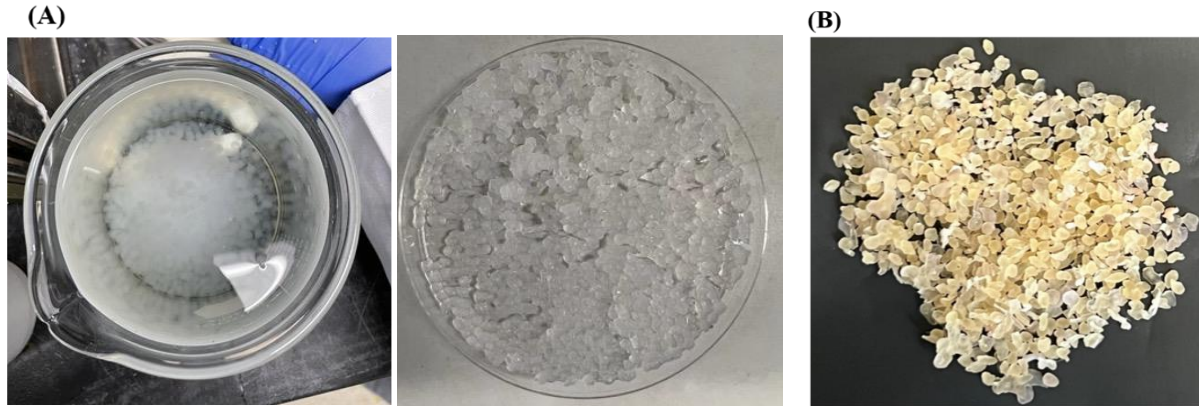
##### *Results:*

1. The growth behavior of encapsulated fungi in the wet state confirms the conclusion that fungal growth is accelerated with an increase in internal nutrient.
2. Upon observation of fungal growth in C2-Cin120-Cout0 and C2-Cin0-Cout1.36, it was observed that the expanded mycelium in C2-Cin0-Cout1.36 was thicker compared to that in C2-Cin120-Cout0. The growth of mycelium in C2-Cin120-Cout0 was primarily concentrated in the surrounding area of the capsule, and the capsule itself exhibited the highest swelling ratio among the contrast groups. This is due to the fact that the growth of encapsulated fungi is influenced by the concentration gradient of nutrients.



**Table 10** Results of Trial 3

	Day 1	Day 3	Day 5	Day 7
C2-Cin0-Cout0				
C2-Cin88.5-Cout0				
C2-Cin100-Cout0				
C2-Cin120-Cout0				
C2-Cin0-Cout1.36				



**Fig. 13** (A) Wet capsules containing a nutrient concentration of 120 g/L; (B) dry capsules

### 2.2.3 Summary of Phase 2 Investigation

Activities in this Phase explored different ways to produce microcapsules containing fungi-based healing agents. From the experimental trials and observations, the optimal microcapsule recipe was identified. In the subsequent phase, capsules that contain a nutrient concentration of 120g/L within each capsule was developed. Figure 14(A) depicts the wet capsules with a nutrient concentration of 120 g/L, while Figure 14(B) shows the capsules in their dry state.

## 2.3 Phase 3: Evaluation of Self-Healing Performance

### 2.3.1 Overview of the research goal

With the appropriate encapsulation technology developed from Phase 2, activities were proceeded to prepare mortar samples containing microcapsules. Subsequently, protocols were developed for the assessment of their self-healing performance.

### 2.3.2 Experimental Design

#### *Preparation of mortar specimens*

Mortar specimens were prepared with ordinary Portland cement and fine river sand following the procedures outlined in ASTM C109. Some samples were combined with fungal capsules, as detailed in Table 11. The mortar mixtures have a cement-water ratio of 0.484. The capsules substituted part of the fine river sand, at a rate determined by the weight ratios of capsule to cement, which were 2%, 3.5%, and 5%, respectively. Table 11 shows the mixture proportions of four groups, including a control mixture without any fungal capsules and three testing mixtures containing 2%, 3.5%, and 5% fungal capsules, respectively. The mixing procedure was modified from ASTM C305. The mixture was conveyed into 2-inch cubic molds and cured at room temperature for 24 hours. After that, the cubic samples were removed from the molds and cured in saturated calcium hydrate solution for a total curing period of 28 days.

**Table 11** Mixture proportion of mortar specimens

Capsule ratio/ %	Cement/g	River sand/ g	Water/ g	Capsules/ g
0	250	687.5	121	0
2	250	682.5	121	5
3.5	250	678.75	121	8.75
5	250	675	121	12.5

### ***Flow table test***

Flow table tests were conducted to examine the flowing property of mortar mixture according to ASTM C1437. A cone frustum mold with a base diameter of 10 cm, an upper diameter of 7 cm, and a height of 5 cm was kept at the center of a clean and dry flow table. Mixtures containing 0%, 2%, 3.5%, and 5% capsules, one mixture per time, were filled in the mold by three layers and tamped each layer for 20 times with a tamping rod. After removing the mold immediately by steady upward pull, the table was raised and drop at 12.5 mm for 25 times immediately. The contact surfaces of the apparatuses are smoothly machined; therefore, it is assumed that there is no frictional intervention between the mold and the flow table surface.

### ***Generation of artificial cracks and healing conditions***

After the curing stage, artificial cracks were generated in order to simulate the deterioration of concrete structures. A rod with a diameter of 0.5 mm was placed on the top surface of both types of mortar samples, with and without fungal capsules, one at a time, to produce concentrated force. During this process, a confined force was applied at both the left and right sides of the mortar samples, to slow the development of cracks and to obtain cracks of different widths. Cracks of three widths were artificially generated in the mortar samples, i.e., narrow cracks (maximum width of single crack is 0 - 0.1 mm), medium cracks (maximum width of single crack is 0.1 mm - 0.4 mm), and wide cracks (maximum width of single crack is larger than 0.4 mm). These three categories were selected following previous studies which reported that narrow cracks with a width below 0.1 mm could be healed autogenously by further hydration [36], and that bacteria-based self-healing technique is inefficient to heal wide cracks ( $> 0.4$  mm) [37]. Therefore, this study examined the effectiveness of the fungi-based self-healing technique in mortar samples with cracks of varying widths and containing different amounts of fungal capsules.

Following the creation of cracks, these two groups of concrete samples, mortar samples containing fungal capsules and control mortar samples, were submerged in PDB solution for 48 hours. Then, the samples were removed from the solution and stored at  $20\text{ }^{\circ}\text{C} \pm 2\text{ }^{\circ}\text{C}$  and relative humidity of  $35\% \pm 3\%$ . Lastly, both the control samples and samples containing fungal capsules were subjected to a 3 mL PDB solution spray on the crack surfaces every three days for a total period of 60 days.

### ***Fourier-transform infrared (FTIR)***

Fourier Transform Infrared (FTIR) tests were conducted with an Agilent Technologies Cary 630 FTIR spectrometer in transmission mode. The spectra were set a range from 400 to  $4000\text{ cm}^{-1}$  with 900 scans. The detected transmission bands indicate the presence of chemical constituents.

### ***Microscope and Scanning Electron Microscope/Energy-Dispersive X-ray Spectrometer (SEM/EDS)***

The Leica EZ4 W stereo microscope with 8x to 35x magnification, 7-way LED illumination, and a 5-megapixel digital camera was utilized to observe the cracked surface that healed by the fungi-based self-healing technique. Crack-filling materials in mortar samples with and without fungal capsules were collected and dried in the oven at  $50\text{ }^{\circ}\text{C}$  for 48 hours. Samples were supper-coated with a 4 nm layer of Pd. Their morphology and elemental composition were characterized by a Hitachi S-2600N scanning electron microscope (1-30 kV) with an energy-dispersive X-ray spectrometer (5-20 kV). A working distance of 4 mm and a voltage of 5 kV were used in SEM testing. A current of  $16\text{ nA}$  and a voltage of 15 kV were set during the EDS analyses.

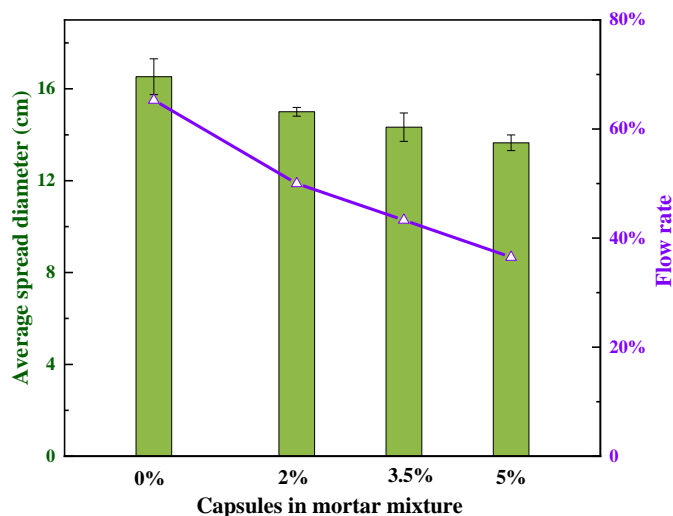
### ***X-ray diffraction (XRD)***

Crack-filling materials in mortar samples containing fungal capsules were collected and dried in the oven at  $50\text{ }^{\circ}\text{C}$  for 48 hours. Dry samples were ground into fine powders to facilitate the analysis. Their phases and crystal orientations were investigated by the Bruker D8 X-ray Diffractometer with Cu radiation. Measurement was made from 10 to 90 degrees with a rate of 2.4 degrees per minute.

### 2.3.3 Experimental Results and Discussions

#### *Workability of mortar mixture containing capsules*

To evaluate the workability of the fresh mortar mixtures under loading impact on a flow table, each mixture, with varying capsule contents, was tested five times. The average spread diameter of each mixture in the flow table test are displayed in Fig. 14, which indicates the flow property and workability. The flow rate is expressed as the percentage increase in spread diameter after raising and dropping the table 25 times over the base diameter of the mold [38]. Fig. 14 demonstrates that the average spread diameter in the control mortar mixture was 16.53 cm. When 2%, 3.5%, and 5% capsules were added, the spread diameters decreased to 15 cm, 14.33 cm, and 13.65 cm, respectively. The flow rates of mortar mixtures ranged between 36.5% and 65.3%, with the flow rate in the control mortar mixture being 65.3%. The incorporation of 2%, 3.5% and 5% capsules in the mortar led to a reduction in flow rate, corresponding to 76.57%, 66.31%, and 55.90% of the rate observed in the control mortar mixture.



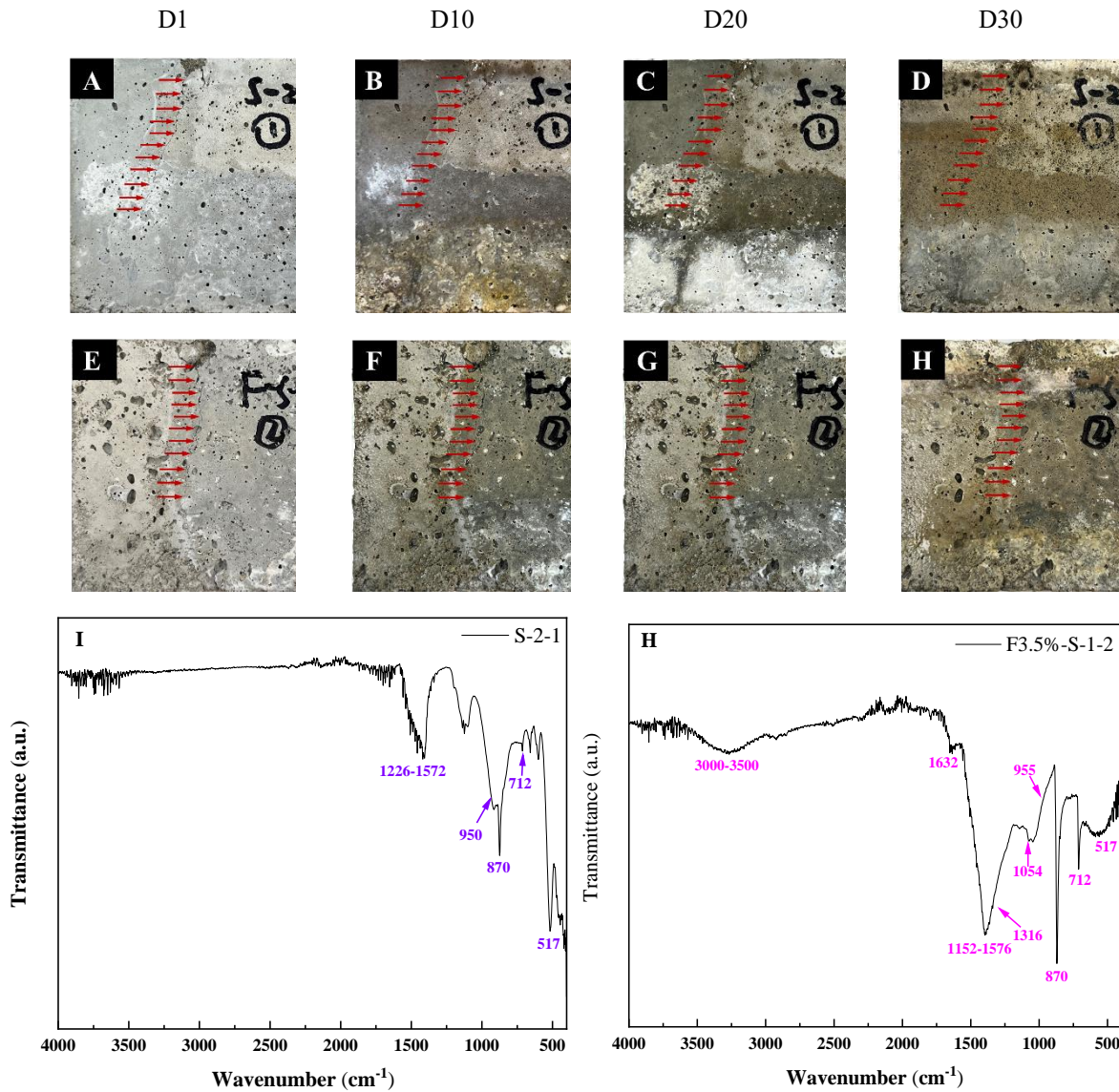
**Fig. 14** Average spread diameter and flow rate in mortar mixture containing capsules

Fig. 14 shows that the contents of capsules contained in the mortar mixture significantly affect the spread of the mixture and its workability. Due to the large particle size of dry capsules, capsules containing fungal cells were used to replace part of the sand particles in the mortar mixture. However, capsules are more sensitive to moisture and absorb more water than river sand. As a result, adding capsules to the mixture reduced the spread diameter and decreased workability. The mortar mixture with capsule contents of 2% and 3.5% resulted in a flow rate of 150 mm and 143 mm, respectively, while the mortar mixture with capsule contents of 5% resulted in a flow rate of 136.5 mm. According to European standard EN 1015-6:1999 [39], a diameter of <140 mm indicates a dry consistency. Therefore, mortar mixture containing 5% capsules would be dry for construction and would require additives to modify its flow properties.

#### *Self-healing performance of narrow cracks (around 0.1mm)*

Alongside workability, the self-healing effectiveness of cracks with different widths was examined. Fig. 15 shows the representative evolution of narrow crack closure in mortar samples without any capsules and with 3.5% fungal capsules, namely in Sample S-2-1 and in Sample F3.5%-S-1-2. The crack closure evolution graph reveals that narrow cracks in both groups of samples were successfully healed after 10 days of treatment.





**Fig. 15** Performance of fungi-based self-healing technique in narrow cracks (A-D) S-2-1, (E-H) F3.5%-S-1-2 at D1, D10, D20, and D30, and (I-J) the IR spectra of S-2-1 and F3.5%-S-1-2

Although narrow cracks were healed in both mortar samples, the healing mechanisms differed. Previous studies have demonstrated that concrete samples containing a large proportion of unhydrated cement, possess the ability to heal narrow cracks through autogenous healing, a natural process that occurs in early-stage concrete without external intervention [40]. When treating cracked samples, moisture, oxygen, and nutrients from the treating solution is drawn into the cracks by capillary action, which promotes continuous hydration and calcium carbonate crystallization. The resulting reaction products, namely calcium silicate hydrate (C-S-H) and calcium carbonate, fill the cracks [41]. However, in mortar samples containing fungal capsules, the treating solution enter the crack space, which promotes the continuous hydration of cement and activates the enclosed fungi. In addition to hydration products of cement, fungal metabolic activities generate filling materials and facilitate the healing process of cracks. Therefore, it is sSeal that the healing process in mortar samples without fungi is primarily attributed to their autogenous healing capacity, whereas in mortar samples with fungi, additional involvement of fungal metabolism contributes to the healing of narrow cracks.

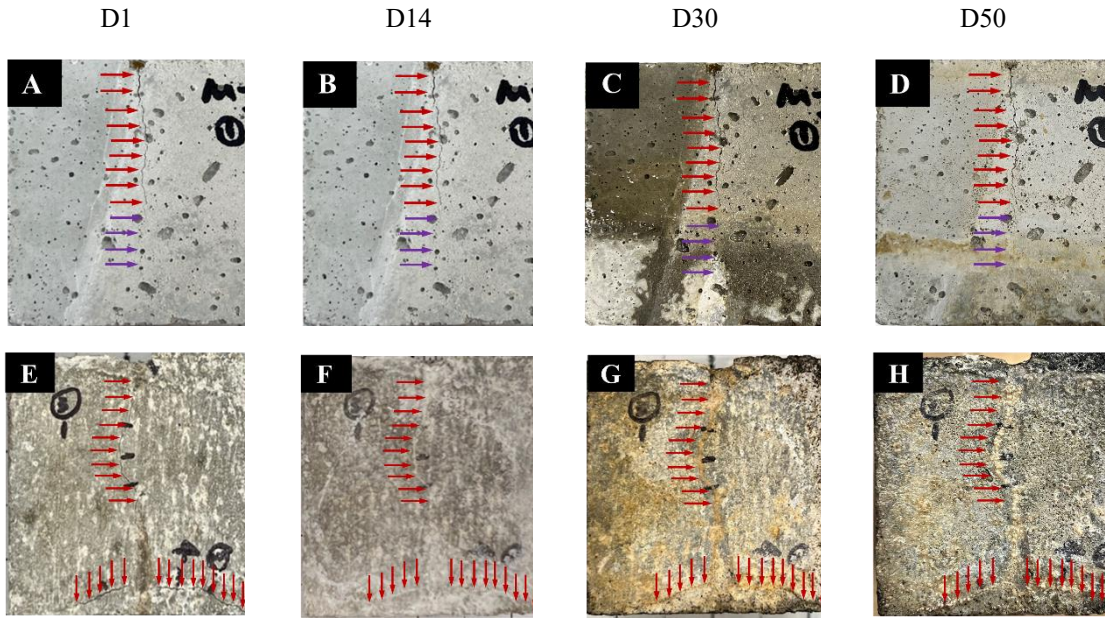
To identify the different healing mechanisms of mortar samples with and without fungi, Infrared (IR) spectroscopy was utilized. The IR spectra (Fig.15 I and H) provide information on the chemical compositions of the crack-filling materials present in S-2-1 and F3.5%-S-1-2. There are indications of autogenous healing in both kinds of samples. Asymmetric Si-O stretching vibrations in C-S-H appear at  $950\text{ cm}^{-1}$  on a shoulder of the broad band in both samples, which

indicates the occurrence of hydration of cement. Both spectra show the bands at  $1437\text{ cm}^{-1}$ ,  $870\text{ cm}^{-1}$ , and  $712\text{ cm}^{-1}$  [34], corresponding to the form of calcium carbonate. Calcium hydrate is one product of hydrated cement, and reacts with carbon dioxide to produce calcium carbonate when exposed to air [42]. The existence of C-S-H and calcium carbonate in both spectra indicates that autogenous healing occurs in both sample S-2-1 and F3.5%-S-1-2. In mortar samples containing fungal capsules, however, in addition to autogenous healing, there is evidence of fungal metabolism which promotes self-healing. One type of fungal metabolism is fungal cell constitution. This can be seen in the broad band ranging from  $3000\text{ cm}^{-1}$  to  $3500\text{ cm}^{-1}$  observed in F3.5%-S-1-2, which is attributed to the presence of fungi [34]. The constitution of fungal cell walls, such as chitin and glycoproteins, display adsorbing and binding capacity of calcium ions, regulating the distribution of  $\text{Ca}^{2+}$  ions [19]. This leads to an increase of  $\text{Ca}^{2+}$  concentration near fungal cell walls, which is the prerequisite for calcium based precipitation [19]. In addition to fungal cell constitution, fungi also produce different types of chemical precipitation that fill cracks through a series of chemical reactions. The first type of chemical precipitation produced by fungi when interacting with mortar samples is calcium carbonate, which is attributed to bands at  $1437\text{ cm}^{-1}$ ,  $870\text{ cm}^{-1}$ , and  $712\text{ cm}^{-1}$ , the same locations as the calcium carbonate produced by autogenous healing [34]. While autogenous healing does generate calcium carbonate, in samples containing fungi, calcium carbonate is created both by autogenous healing and by fungi related mechanisms. The physicochemical degassing of  $\text{CO}_2$  gas produced by fungal respiration occurs in a solution as  $\text{H}_2\text{CO}_3$ ,  $\text{HCO}_3^{2-}$ , and  $\text{CO}_3^{2-}$ . This process is known to be influenced by the carbonate alkalinity. The  $\text{Ca}^{2+}$  ions that are bound to the surface of the fungal cell wall react with these carbonate species, resulting in the generation of calcium carbonate on the surface of the fungal cell walls. The second type of chemical precipitation is calcium oxalate. The peak at  $1316\text{ cm}^{-1}$  falls in the range of  $1152\text{--}1576\text{ cm}^{-1}$  in F3.5%-S-1-2, which is attributed to the symmetric vibrations of oxalate group. The existence of calcium oxalate also contributes to the band at  $955\text{ cm}^{-1}$  and  $1632\text{ cm}^{-1}$  in the spectrum of F3.5%-S-1-2. While calcium carbonate can be created by autogenous healing, these bands indicate the chemical precipitation of calcium oxalate that is uniquely produced by fungi-based self-healing technique. Fungi produce a variety of organic acids, among of which oxalic acid is one of the most common [19]. Oxalic acid is prone to precipitate in the form of calcium oxalate crystals due to interactions between fungi and calcium-rich concrete [34]. The presence of functional groups in F3.5%-S-1-2, such as oxalate, highlights the difference in crack healing between mortar samples without and with fungal capsules, indicating the effect of fungi-based self-healing technique. Therefore, only autogenous healing is found in mortar samples without fungi. The fungi-based self-healing technique in F3.5%-S-1-2 contributes to the additional healing effects, i.e., the growth of fungal fibers and the generation of chemical precipitation, facilitating the healing of narrow cracks.

#### ***Self-healing performance of medium cracks (between 0.1mm to 0.4mm)***

The effect of fungi-based self-healing is even more pronounced in the mortar samples with medium and wide cracks. The closure evolution of medium and wide cracks was observed visually and by measuring the crack width at different treatment periods. The results show that in mortar samples without fungi, medium cracks healed slowly (Fig. 16 A-D). Upon naked-eye observation of sample M-3-1, only the tips of the cracks were completely healed, because of their smaller size. This was attributed to autogenous healing, similar to the self-healing of narrow cracks. However, the remaining parts of medium cracks were unhealed. This indicates that autogenous healing is inefficient in healing medium cracks. By contrast, in the sample containing 2% fungal capsules, cracks with width of 0.1-0.4 mm were completely healed after 14 days of treatment. Moreover, after these cracks were completely healed, the fungi-based self-healing technique exhibited an additional advantage not seen in other self-healing methods. Fungal mycelium covered the surface of the cracks and the surrounding surface area of the mortar samples after 30 days (as shown in Fig. 16G). After this stage, the mycelium on the surface of the mortar samples became thicker. These results indicate that fungi-based self-healing is more effective in healing medium-sized cracks compared to the healing process in mortar samples without fungi, due to both fungal growth and fungi-induced precipitation in the self-healing process.

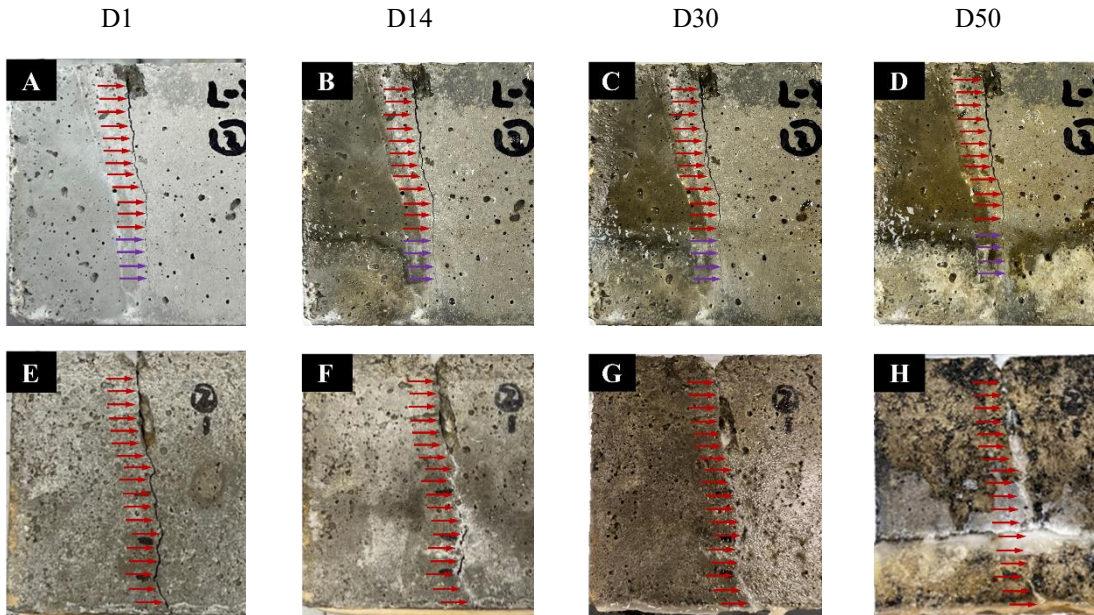


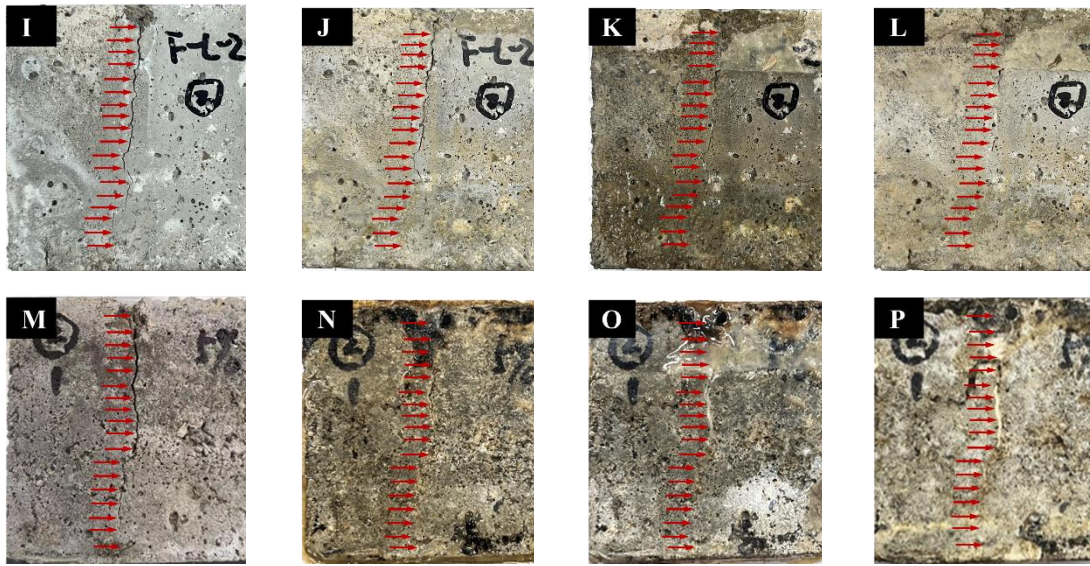


**Fig. 16** Performance of fungi-based self-healing technique in medium cracks at D1, D14, D30, and D50 (A-D) M-3-1 and (E-H) F2%-M-3-1

#### *Self-healing performance of wide cracks (over 1 mm)*

Much like in medium crack, regular mortar with wide crack exhibited a similar slow healing process, in which only the tip area of the crack (indicated by the purple arrow in Fig.17 A-D) healed in the mortar samples without fungi. The rest of the wide crack control group samples remained unhealed. By contrast, mortar samples containing fungal capsules repaired wide cracks with an average width over 0.4 mm more effectively compared to the control group. After 14 days, white precipitation was observed in specific regions of the crack spaces in mortar samples containing capsules, especially at the tip of cracks. This precipitation indicates that the healing of cracks initiates from the narrowest area, which is easier to heal.





**Fig. 17** Performance by fungi-based self-healing technique in wide cracks (A-D) L-3-2, (E-H) F2%-L-2-1, (I-L) F3.5%-L-2-2, and (M-P) F5%-L-2-1

In term of healing performance, in the mortar samples containing 2% and 3.5% capsules only the tip areas were healed (Fig.17 F and J), whereas in samples containing 5% capsules, the healing extended beyond the tip along the cracked space (Fig.17 N). After 30 days, in samples containing 2% and 3.5% capsule, white fungal fibers were visible, and in samples containing 5% capsules a broader area was covered with white fungal fibers. The development of white fungal fibers was independent of the crack width, because in addition to the tip area, fungal fibers were also observed in the middle area of crack in samples containing 2% capsules, and in the top area of crack in samples containing 3.5% capsules. Additionally, a broader area was covered by white fungal fibers in samples containing 5% capsules at the same period. After 50 days, white mycelium growth covered nearly all crack spaces and surrounding areas in all samples containing capsules.

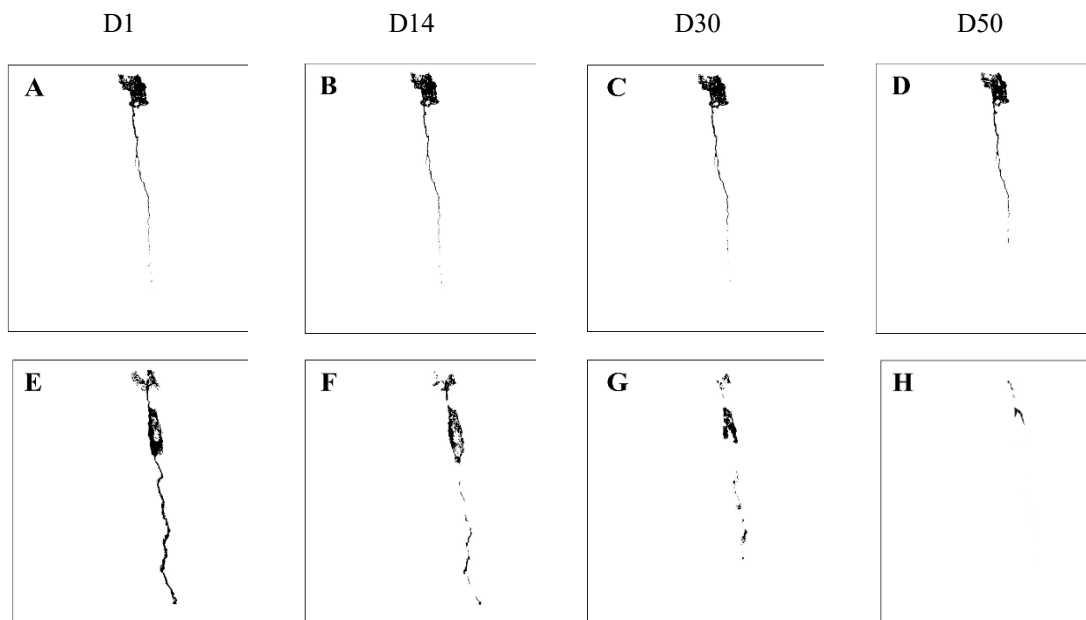
#### 2.3.4 Analyses of Experimental Observations

The healing of medium and wide cracks in mortar samples containing fungi is characterized by a two-stage process. During the first stage, fungi are released from broken capsules and germinate in the crack space, producing chemical precipitation to initiate the healing process. However, the development of mycelium is restricted by the limited availability of oxygen and nutrients in the crack space. Once the crack space is almost filled with fungal fibers and precipitation, the second stage commences. In this stage, fungi have unrestricted access to oxygen, facilitating significant mycelium development. As a result, the mycelium forms a cover over the crack space and the surrounding surface of the mortar. The surface of fungal mycelium displayed hydrophobic properties, which would improve the water-tightness of the mortar samples [34]. This two-stage process in fungi-based self-healing is beneficial for healing wide cracks in concrete structures. Self-healing of wide cracks in concrete is always a challenging task [37]. The technology of self-healing based on bacteria also presents limitations when it comes to repairing wide cracks in concrete. The reason for this is that repairing wide cracks requires a significant amount of calcium carbonate precipitates to be generated within a relatively short period. The bacterial cell walls are negatively charged and serve as nucleation sites for the bacteria-induced precipitation of calcium carbonate, which is typically positively charged [43]. The nucleation sites on the surface of bacterial cell walls are insufficient to promote complete healing of wide cracks. In addition, bacteria are unable to reach the far regions of the wide cracks, because of their limited ability to transport bacterial cells and nutrients to the affected area. This is particularly challenging for wide cracks, where the distance between the outer and inner surfaces of the crack may be significant. Fungal unique qualities could overcome these limitations faced by bacteria-based self-healing technology in healing wide cracks. One of the key advantages of fungi is their ability to offer sufficient nucleation sites for calcium-based precipitation. The 3D structure of fungal mycelium exhibits a large surface-to-volume ratio, which provides a large number of nucleation sites for chemical precipitation. Another of the key advantages of fungi is their interconnected structures. The fungal cells used in this study grow as elongated structures and form a 3D networked mycelium material. This structure bridges the

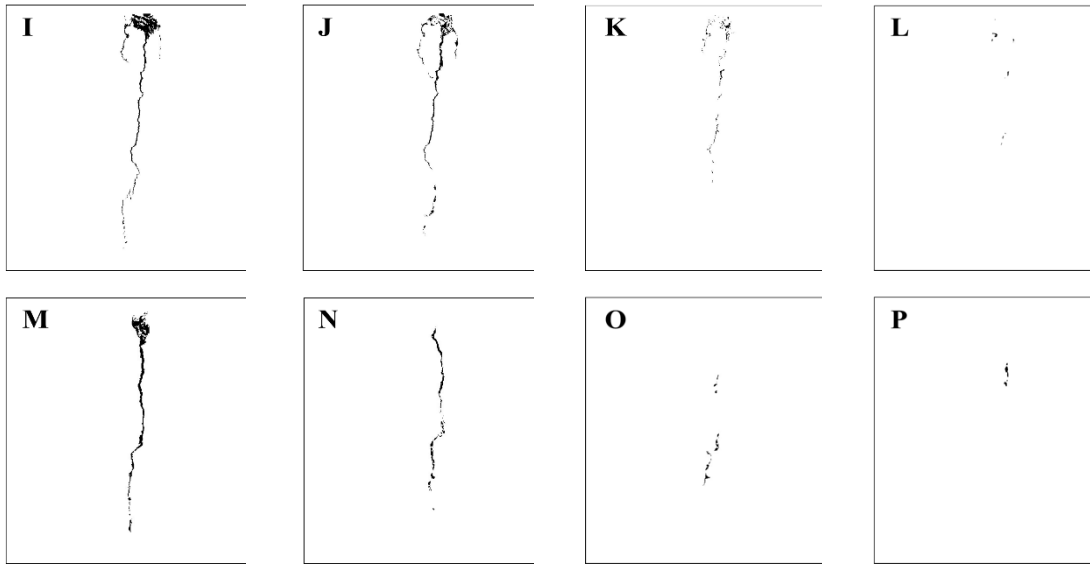
cracked sides and facilitates the healing process of the cracks. Therefore, the two-stage healing process in fungi-based self-healing include both the development of fungal mycelium and fungi-induced precipitation, providing significant advantages for repairing wide cracks in concrete structures.

### ***Impact of different concentration of fungal healing microcapsules***

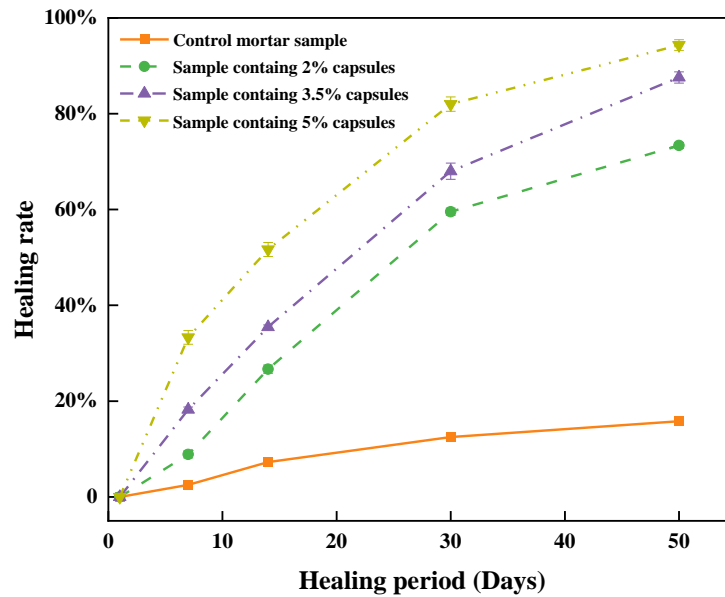
The self-healing capacity of mortar samples could be enhanced by incorporating fungal capsules, which has already been demonstrated in pervious sections. This section investigates the impact of different ratios of fungal capsules that was incorporated in mortar samples on the self-healing performance of mortar samples, especially in the mortar samples that have wide cracks. In order to evaluate the impact, the images presented in Figure 17 were converted to binary form. Fig. 18 presents the binary images of cracks in the mortar samples containing varying ratios of capsules. The healing rate is defined as the ratio of the closed area to the original surface area of the crack. Figure 19 shows the healing rate in more samples at different healing periods. These results show that the cracks were observed to gradually heal over time. In control mortar samples, the healing rate was initially slow during the first 14 days and slowly increase to 50 days. The healing rate reaches a plateau after 50 days. However, in the mortar samples containing fungal capsules, the healing rate was slow during the first 7 days. The healing rate exhibited a linear increase from 7 to 30 days, followed by a slower increase in the healing rate after this period. Based on visual observation, the healing progress remained nearly unchanged after 50 days. Another observation from the results is that the addition of fungal capsules led to an earlier onset of the healing process and an increase in the healing rate. Specifically, the presence of these fungal capsules allowed for a faster and more effective repair of the wide cracks in the mortar samples. Increasing the contents of fungal capsules in mortar samples significantly improved the healing rate. Only 15.8% of wide cracks were healed in the control mortar samples. However, the addition of capsules improved the healing rates to 464%, 554%, and 597% times that of the control samples when 2%, 3.5% and 5% of capsules were added, respectively. This result indicates the high effectiveness of fungi-based self-healing. Higher healing rate was observed in mortar samples containing more capsules. The higher content of capsules in the samples results in a larger number of capsules being available in the cracked area, which increases the number of healing start spots within the cracks and initiates a more robust healing process.







**Fig. 18** Binary images of mortar samples with different crack sizes after different repair time: (A-D) L-3-2, (E-H) F2%-L-2-1, (I-L) F3.5%-L-2-2, and (M-P) F5%-L-2-1



**Fig. 19** Healing percentage of initial cracks width in mortar samples containing different contents of fungal capsules

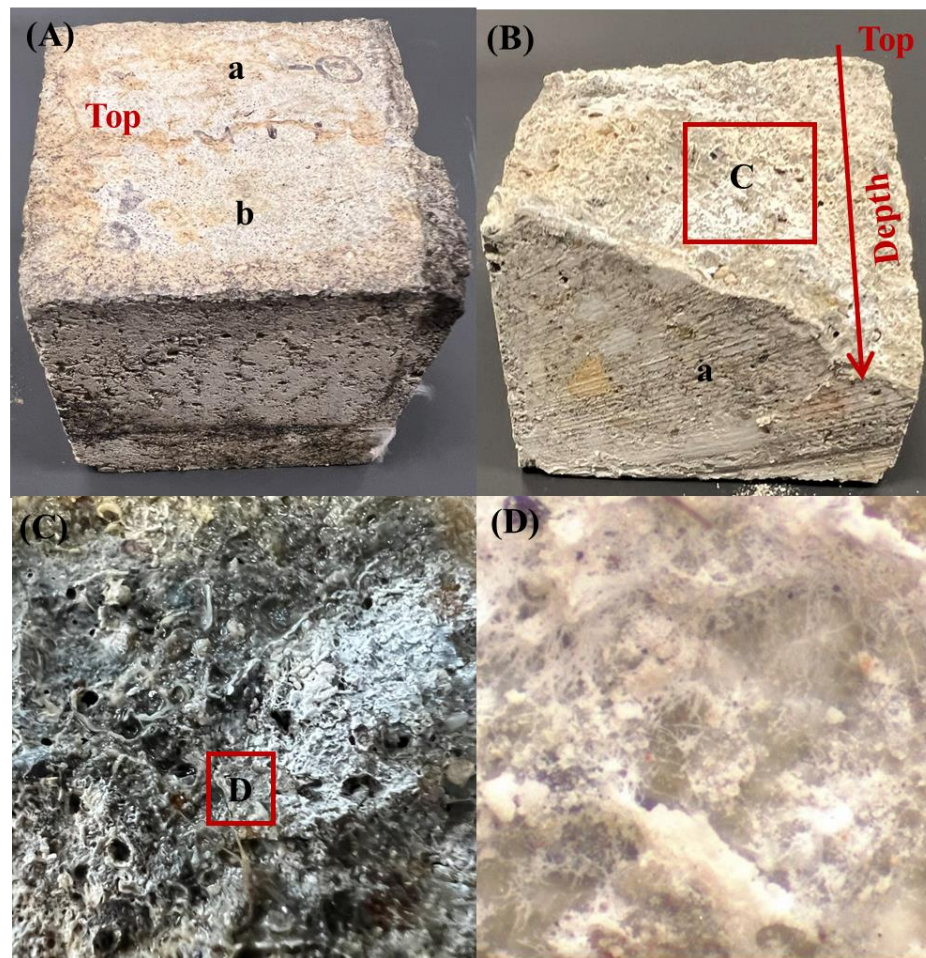
### ***Mechanism of encapsulated fungi-based self-healing***

The discussion of fungi-based self-healing mechanism already demonstrated its distinction from autogenous healing. Discussing morphology and crystalline information of the crack-filling materials can provide further information regarding the effectiveness of encapsulated fungi-based self-healing technique. The morphology of healed surfaces in samples containing fungal capsules was examined both by naked eye observation and under an optical microscope. Naked eye observations of the surface provide a quick and initial assessment of healing progress in cracks. Moreover, an optical microscope offers a detailed analysis of the morphology and distribution of fungal growth within the healed areas.

The healed sample F5%-M-1 (Fig.20 A) was cut through the healed surface into the deep cracked surface, as shown in Fig.20 (B-D). Both intact capsules and broken capsules were observed on the cracked surface. Around these capsules, several large areas of chemical precipitation (white color) were found in the fungi-based mortar sample (gray color), which

is clearly seen by the naked eye (Fig. 20C). These observations demonstrate that the encapsulated fungi-based self-healing process initiates from the generation of cracks. When the mortar is damaged, some capsules rupture, releasing the fungal spores and nutrients, which then grow and produce precipitation. Other capsules remain intact, and they also have access to oxygen and moisture, developing fungal fibers and precipitation. These fungal fibers and precipitation fill the cracks and ultimately restore the integrity of the mortar samples.

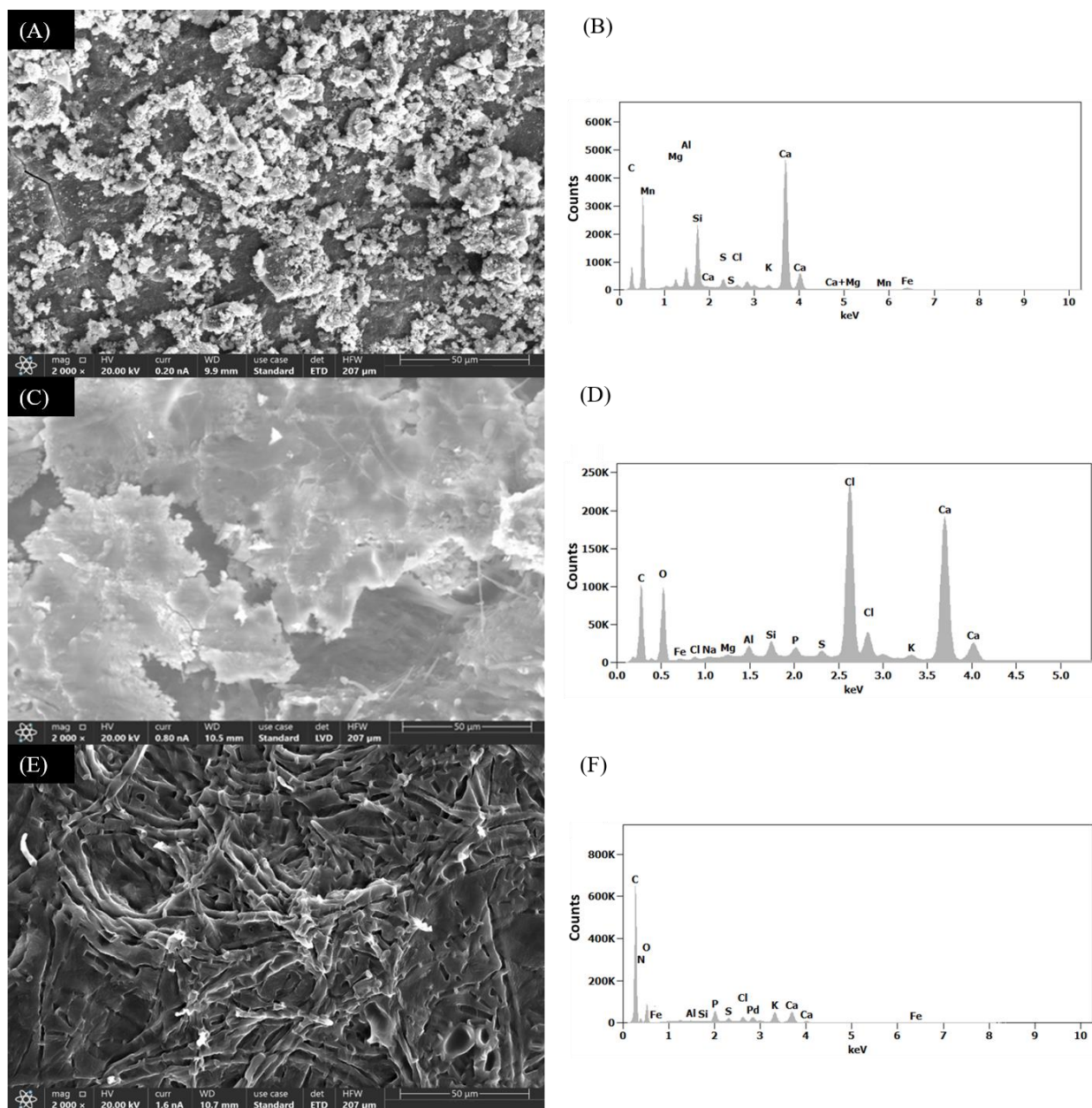
Based on the optical microscopy images, a filamentous mycelial network containing numerous fungal hyphae was developed on the healed surface and minerals were produce in the surrounding area (Fig. 20D). Fungal fibers were distributed uniformly throughout the healed area, including the depth of the crack. This uniform distribution of fungal fibers is effective in three ways: first, the far-reaching mycelial network forms a strong and resilient bond with the surrounding material. Second, fungal fibers penetrate and fill the voids and cavities within the cracks, reducing water infiltration and improving durability. Third, fungal fibers penetrate into the deep crack space or bridge wide-spaced cracked surfaces, where other self-healing mechanisms such as bacteria-based self-healing is limited in their ability to fill the entire volume of the crack.



**Fig. 20** (A) Fungi-based self-healing mortar sample (F5%-M-2-1); (B) Split the sample along the healed crack surface; (C) Captured image with x3 magnification; (D) Microscopy image with x3500 magnification

Fig. 21 (A-D) show the SEM images and EDX analysis of crack-filling materials on self-healed surface in S-2-1 and in F5%-M-2-1. Fig. 21E illustrates the morphology of the fungal mycelium that covered on the surface of F5%-M-2-1. Fig. 21A shows the microstructure of the self-healed crack surface in sample S-2-1, where the self-healing substances are dispersed on the crack surface. Through EDX analysis, it was found that the crack-filling materials in the control mortar samples were composed of calcium (Ca), magnesium (Mg), aluminum (Al), and silicon (Si), which are the main components of Portland cement or its hydration products. In the mortar samples containing fungal capsules, the healing substances were found to be mainly composed of calcium (Ca), carbon (C), and oxygen (O). The intensities of magnesium

(Mg), aluminum (Al), and silicon (Si) were found to be weaker in the fungal-containing mortar samples compared to the control samples. This indicates that the crack-filling materials in the fungal-containing samples cannot be solely attributed to cement hydration and autogenous healing. These findings suggest that the self-healing process in the fungal capsule-containing mortar samples differs from that in the control samples and is primarily due to the precipitation induced by the fungi. The crack-filling materials in the sample F5%-M-2-1 is much thicker than that in the sample S-2-1. Thick precipitation around fungal fibers were observed in Fig. 22C, which also indicates the self-healing production is attributed to fungal metabolism. Considerable fungal fibers were found on the surface of mortar samples containing fungal capsules (Fig. 22E). Compared to the fungal fibers grown in the crack spaces, the limited availability of Ca source on the top surface of mortar samples results in a low intensity of Ca in Fig. 22F.

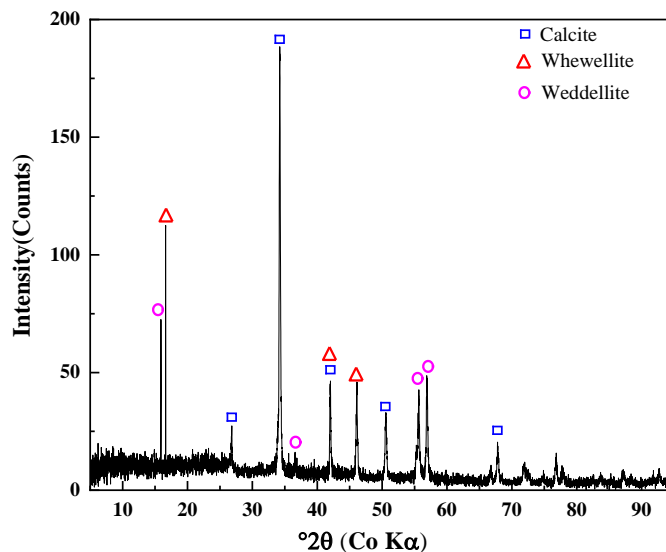


**Fig. 22** SEM images and EDX analysis of healed concrete samples from (A-B) S-2-1 self-healed crack surface; (C-D) F5%-M-2-1 self-healed crack surface; (E-F) F5%-M-2-1 surface covered by fungal mycelium

Alongside morphology, crystalline phases play a significant role in clarifying the fungi-based self-healing mechanism. Although the chemical compositions have been demonstrated by the spectra of FTIR, the crystalline phases of chemical precipitation caused by fungi-based self-healing technique requires further analysis. An XRD test was conducted to observe



the crystalline information of the precipitation produced by the fungi-based self-healing technique that fills in the crack space. The XRD pattern of the fungi-based self-healing mortar sample is shown in Figure 23. By analyzing the peaks in the XRD pattern, it identifies the crystalline phases present in the fungi-based self-healing production. The X-ray diffraction (XRD) pattern of the sample revealed prominent peaks at  $2\theta$  angles of  $23.03^\circ$ ,  $35.94^\circ$ ,  $43.12^\circ$ , and  $69.11^\circ$ , which can be attributed to the crystal plane of calcite. The characteristic peaks observed at  $2\theta$  angles of  $16.97^\circ$ ,  $43.98^\circ$ , and  $45.77^\circ$  correspond to the crystal plane of whewellite. Similarly, the peaks observed at  $2\theta$  angles of  $15.98^\circ$ ,  $21.81^\circ$ ,  $33.19^\circ$  and  $41.99^\circ$  are associated with the crystal plane of weddellite [44]. The XRD testing results indicate the high intensity and peaks of calcite, whewellite and weddellite in mortar samples containing fungal capsules. This information determined the composition of the fungi-based self-healing products contains crystalized calcite, whewellite, and weddellite. In addition, their crystalized structures contribute to the long-term strength of self-healing products in the healed cracks.



**Fig. 23** XRD pattern of self-healing production in mortar sample containing fungal capsules (F5%-M-1)

### 2.3.4 Summary of Phase 3 Investigation

Activities in this stage investigated the self-healing performance of fungi-mediated technology in alkaline mortar samples. The workability of mortar mixture containing different contents of fungal capsules was studied by conducting flow table tests. Cracks with three widths, i.e., narrow cracks, medium cracks, and wide cracks, were generated in mortar samples containing different contents of fungal capsules. Their healing process was investigated by visual observation and micro-scale characterization.

Flow table tests demonstrate that with 2%, 3.5%, and 5% capsules in mortar specimens, the flow rate was decreased to 76.57%, 66.31%, and 55.90% of the rate in the control mortar mixture. The addition of 5% or more fungal capsules to a mixture might require the inclusion of additives to enhance its flow properties.

Cracks with a width narrower than 0.1 mm were healed in both the control samples and fungi-based self-healing mortar samples. FTIR tests show that the healing in the control samples was attributed to autogenous healing, while in fungi-based self-healing mortar samples, both autogenous healing and fungal metabolism were involved.

Fungi-based self-healing technique is able to heal cracks wider than 0.1 mm, unlike control samples where only autogenous healing occurs, which fail to heal such cracks.

A two-stage self-healing process was observed in mortar samples with cracks wider than 0.1 mm. In the first stage, fungi-based self-healing repairs cracks with widths of 0.1-0.4 mm completely after 14 days; and repair 90% of the area of cracks wider than 0.4 mm after 30 days. In the second stage, hydrophobic fungal mycelium covers the surface of the cracks



and partially covers the surrounding surface of mortar samples, which offer an additional advantage of reducing water infiltration and prolonging durability of structures.

When considering the impact of varying fungal capsule contents on healing performance, it is notable that the incorporation of microcapsules led to a substantial improvement in healing rates. While the control mortar samples exhibited a low healing rate of 15.8% for wide cracks, the healing rates were increased by 464%, 554%, and 597% times that of the control samples with the addition of 2%, 3.5%, and 5% capsules, respectively.

## PLANS FOR IMPLEMENTATION

The research team has proactively disseminated the research's progress at various professional venues, such as the TRB annual conference, the annual workshop by the US DOT National University Transportation Center on Infrastructure Renewal and Life Extension (TriDurLE), and local ACI chapter events.

The research team has initialized discussions with University utilities, State DOTs, and industry to explore opportunities for future field demonstration of the technology. The dialogues also included Ohio Concrete, Master Builder Chemicals (a leading construction chemical supplier, previously part of BASF construction division). Issues with concrete cracks are prevalent in transportation assets. Innovative technology based on this proof-of-concept study has broad ramifications. The research team will work closely with Ohio DOT on opportunities to the further implementation of field demonstration.

The research team has worked closely with Case Western Reserve University Technology Transfer Office (TTO), which has track record in successfully facilitating technology translation activities. A U.S. patent application has been filed for this invention. Under the guidance of TTO technology advisor, the team has proactively engaged in discussions with potential vendors who are interested to joint develop or license the technology. As this technology has potential benefits for transportation infrastructure nationwide, commercial pathways will be developed under the guidance of TTO to fully explore commercialization opportunities.

This Type 1 project has successfully proven the feasibility of fungi-based self-healing technology concept. The results show that cracks over 1mm were successfully healed with the fungi-based healing agents developed from this project. The performance is superior to existing self-healing technologies. Besides, the healed concrete surface features super-hydrophobicity, which prevent the ingress of water and corrosive ions. Scalable production procedures have been developed to produce microcapsules containing fungi-based healing agents. This set the basis for further technology development and demonstration.

Leveraging the discoveries in this NCHRP-IDEA Type 1 project, the research team plans to explore an NCHRP-IDEA Type 2 project to further the development of the technology, which will constitute to work with industry partners and government agency to upscale the production of self-healing microcapsules, develop design recipe to incorporate self-healing agents, and evaluate the endurance of the self-healing performance. The team will also work with these partners to jointly implement technology demonstration.

## CONCLUSIONS

This project successfully explored the concept of an innovative fungi-based self-healing concrete technology. The results show promising potentials.

*Phase 1* of the project focused on study of fungi-mortar surface interactions. Experiments were conducted to inoculate fungi on the surface of mortar samples and the growth behaviors of fungi were observed. The results showed that fungi was able to germinate on the surface of mortar and showed rapid growth behaviors in covering the surface with mycelium fibers. However, the mycelium development was influenced by the pH value, with high pH delays the germination time and increased the mature time (defined in this paper as the time that mycelium completely covers the surface of mortar). Under favorable conditions, fungi covered a surface area of mortar 86 times the area of the original fungi inoculum after 96 hours. Such fast growth of fungi would contribute to high efficiency in healing cracks.

The microscopic characteristics of fungi mycelium were analyzed with advanced instrument such as SEM/EDS, and FTIR. The SEM images confirmed that fungi was able to germinate spores and develop mycelium despite of the high pH value on mortar surface. Fungal mycelium is able to precipitate calcium minerals, which would contribute to healing cracks. The FTIR spectra confirmed the presence of calcium carbonate and calcium oxalate monohydrate, which are the resultants of the metabolism by fungi.

The fungal mycelium grown on the surface of mortar was observed to be hydrophobic with an average contact angle of  $134.92^\circ$ . The hydrophobic behavior would lead to higher water repellency and reduce water infiltration into concrete through the cracks. Analyses based on the experimental observations show that fungi feature much higher potential healing efficiency compared with bacteria.

To ensure longevity and sustainability of self-healing function, *Phase 2* explored the development of microcapsules to shield the fungi spores. Different methods were studied to produce microcapsules containing fungi-based healing agents. From the experimental trials and observations, the optimal microcapsule recipe was identified. Procedures and equipment to produce microcapsules were developed which features excellent scalability.

Activities in *Phase 3* investigated the self-healing performance of fungi-mediated technology in alkaline mortar samples. The workability of mortar mixture containing different contents of fungal capsules was studied by conducting flow table tests. Cracks with three widths, i.e., narrow cracks, medium cracks, and wide cracks, were generated in mortar samples containing different contents of fungal capsules. Their healing process was investigated by visual observation and micro-scale characterization. The developed self-healing microcapsules was found to efficiently heal cracks with a wide ranges of sizes. Besides, hydrophobic fungal mycelium covers the surface of the cracks and offers an additional advantage of reducing water infiltration and prolonging durability of structures.

Overall, the research activities successfully proof the concept of the innovative seal-healing technology. Highlights of major aspects of this new technology include:

- *Superior self-healing performance:* The fungi self-healing agent successfully healed cracks in a cement mortar mix as wide as 1mm, which is well beyond the state of the art in the self-healing technologies (heal cracks no more than 0.45mm).
- *Excellent water tightness:* The surface of concrete treated with fungi features high hydrophobicity, which helps to mitigate concrete deterioration associated with water and ion ingress and the subsequent damages such as corrosion, scaling, etc.
- *Scalability:* protocol for microcapsule production is scalable for mass production and produces microcapsules that give consistent self-healing performance.

The success in this proof-of-concept study lays down the foundation for further development and demonstration of this innovative self-healing concrete technology.

## INVESTIGATORS' PROFILES

Dr. Xiong (Bill) Yu (PI): the Opal J. and Richard A. Vanderhoof professor and chair, Department of Civil and Environmental Engineering, Case Western Reserve University (CWRU). Dr. Yu's research aims at understanding the multiscale multiphysics processes in geomaterials and geosystems, designing of multifunctional smart materials, bio-mediated and bio-inspired engineering, intelligent infrastructure systems, etc. He has published over 150 journal papers and 200 conference proceedings. Many received recognitions as best paper awards or highlighted by ASCE magazine and TRB newsletters. He closely integrates his research with education, mentoring, and outreach activities. He has pioneered the study of fungi concrete interaction for concrete healing, soil improvements, and have published extensively in the related areas.

The project team also includes *Dr. Xijin (Emma) Zhang* (Postdoctoral Associate and Adjunct Assistant Professor at Case Western Reserve University, Assistant Professor at George Mason University since Fall 2023), with expertise in construction materials, fiber reinforced concrete, and multifunctional concrete materials; *Rodrigo Teixeira Schossler* (Ph.D. student at Case Western Reserve University), with expertise in concrete material design and testing, machine learning (ML) and artificial intelligence (AI) for concrete design, performance assessment; *Qammar Abbas* (Ph.D. student at Case Western Reserve University), with expertise in concrete materials and biomedicated construction materials.

## REFERENCES

1. Jonkers, H.M., *Bacteria-based self-healing concrete*. Heron, 56 (1/2), 2011.
2. Wiktor, V. and H.M. Jonkers, *Quantification of crack-healing in novel bacteria-based self-healing concrete*. Cement and Concrete Composites, 2011. **33**(7): p. 763-770.
3. Bhaskar, S., et al., *Effect of self-healing on strength and durability of zeolite-immobilized bacterial cementitious mortar composites*. Cement and Concrete Composites, 2017. **82**: p. 23-33.
4. Achal, V., A. Mukerjee, and M.S. Reddy, *Biogenic treatment improves the durability and remediates the cracks of concrete structures*. Construction and Building Materials, 2013. **48**: p. 1-5.
5. Van Tittelboom, K., et al., *Use of bacteria to repair cracks in concrete*. Cement and Concrete Research, 2010. **40**(1): p. 157-166.
6. De Muynck, W., et al., *Bacterial carbonate precipitation improves the durability of cementitious materials*. Cement and concrete Research, 2008. **38**(7): p. 1005-1014.
7. Jonkers, H.M., et al., *Application of bacteria as self-healing agent for the development of sustainable concrete*. Ecological engineering, 2010. **36**(2): p. 230-235.
8. Vijay, K., M. Murmu, and S.V. Deo, *Bacteria based self healing concrete—A review*. Construction and building materials, 2017. **152**: p. 1008-1014.
9. Jackson, S. and I. Heath, *Roles of calcium ions in hyphal tip growth*. Microbiology and Molecular Biology Reviews, 1993. **57**(2): p. 367-382.
10. Riquelme, M., *Tip growth in filamentous fungi: a road trip to the apex*. Annual review of microbiology, 2013. **67**: p. 587-609.
11. Bartnicki-García, S., *Hyphal tip growth: outstanding questions*. Mycology Series, 2002. **15**: p. 29-58.
12. Gow, N.A. and G.M. Gadd, *Growing fungus*. 2007: Springer Science & Business Media.
13. Girometta, C., et al., *Physico-mechanical and thermodynamic properties of mycelium-based biocomposites: a review*. Sustainability, 2019. **11**(1): p. 281.
14. TEIXEIRA, L., L. Coelho, and N.D. Tebaldi, *CHARACTERIZATION OF Fusarium oxysporum ISOLATES AND RESISTANCE OF PASSION FRUIT GENOTYPES TO FUSARIOSIS*. Revista Brasileira de Fruticultura, 2017. **39**(3).
15. Smith, S.N. and W. Snyder, *Germination of Fusarium oxysporum Chlamydospores in Soils Favorable*. Phytopathology, 1972. **62**: p. 273-277.
16. Gordon, T.R., *Fusarium oxysporum and the Fusarium wilt syndrome*. Annual review of phytopathology, 2017. **55**: p. 23-39.
17. Legodi, M., et al., *Rapid determination of CaCO<sub>3</sub> in mixtures utilising FT—IR spectroscopy*. Minerals engineering, 2001. **14**(9): p. 1107-1111.
18. Lin, M.-H., et al., *Quantitative analysis of calcium oxalate hydrate urinary stones using FTIR and 950/912 cm<sup>-1</sup> peak ratio*. Vibrational Spectroscopy, 2019. **102**: p. 85-90.
19. Bindschedler, S., G. Cailleau, and E. Verrecchia, *Role of fungi in the biomineralization of calcite*. Minerals, 2016. **6**(2): p. 41.
20. Di Giambattista, L., et al., *New marker of tumor cell death revealed by ATR-FTIR spectroscopy*. Analytical and bioanalytical chemistry, 2011. **399**(8): p. 2771-2778.
21. Wang, J., et al., *Self-healing concrete by use of microencapsulated bacterial spores*. Cement and concrete research, 2014. **56**: p. 139-152.
22. Al-Kheetan, M.J., M.M. Rahman, and D.A. Chamberlain, *Moisture evaluation of concrete pavement treated with hydrophobic surface impregnants*. International Journal of Pavement Engineering, 2019: p. 1-9.
23. Ramachandran, R., K. Sobolev, and M. Nosonovsky, *Dynamics of droplet impact on hydrophobic/icephobic concrete with the potential for superhydrophobicity*. Langmuir, 2015. **31**(4): p. 1437-1444.
24. Feeney, D.S., et al., *Three-dimensional microorganization of the soil–root–microbe system*. Microbial ecology, 2006. **52**(1): p. 151-158.

25. Hallett, P.D. and R. Gaskin. *An introduction to soil water repellency*. in *Proceedings of the 8th International Symposium on Adjuvants for Agrochemicals (ISAA2007)*. 2007. International Society for Agrochemical Adjuvants (ISAA) Columbus, Ohio, USA.
26. Pelishek, R., J. Osborn, and J. Letey, *The effect of wetting agents on infiltration*. Soil Science Society of America Journal, 1962. **26**(6): p. 595-598.
27. Smyl, D., F. Ghasemzadeh, and M. Pour-Ghaz, *Modeling water absorption in concrete and mortar with distributed damage*. Construction and Building Materials, 2016. **125**: p. 438-449.
28. Zhao, H., et al., *Influence of pore structure on compressive strength of cement mortar*. The Scientific World Journal, 2014. **2014**.
29. Bang, S.S., J.K. Galinat, and V. Ramakrishnan, *Calcite precipitation induced by polyurethane-immobilized Bacillus pasteurii*. Enzyme and microbial technology, 2001. **28**(4-5): p. 404-409.
30. Soysal, A., et al., *Evaluating the self-healing efficiency of hydrogel-encapsulated bacteria in concrete*. Transportation Research Record, 2020. **2674**(6): p. 113-123.
31. Gao, M., et al., *Immobilized bacteria with pH-response hydrogel for self-healing of concrete*. Journal of environmental management, 2020. **261**: p. 110225.
32. Fahimizadeh, M., et al., *Biological self-healing of cement paste and mortar by non-ureolytic bacteria encapsulated in alginate hydrogel capsules*. Materials, 2020. **13**(17): p. 3711.
33. Tang, Y. and J. Xu, *Application of microbial precipitation in self-healing concrete: A review on the protection strategies for bacteria*. Construction and Building Materials, 2021. **306**: p. 124950.
34. Zhang, X., et al., *Study on the behaviors of fungi-concrete surface interactions and theoretical assessment of its potentials for durable concrete with fungal-mediated self-healing*. Journal of Cleaner Production, 2021. **292**: p. 125870.
35. Zhang, X., et al., *Development and characterization of novelly grown fire-resistant fungal fibers*. Scientific Reports, 2022. **12**(1): p. 10836.
36. Reinhardt, H.-W. and M. Jooss, *Permeability and self-healing of cracked concrete as a function of temperature and crack width*. Cement and concrete research, 2003. **33**(7): p. 981-985.
37. Paine, K. *Bacteria-based self-healing concrete: Effects of environment, exposure and crack size*. in *Proceedings of the RILEM Conference on Microorganisms-Cementitious Materials Interactions*. 2016. RILEM Publications SARL Paris, France.
38. Giaccio, G. and R. Zerbino, *Optimum superplasticiser dosage for systems with different cementitious materials*. Indian Concrete Journal, 2002. **76**(9): p. 553-557.
39. Alonso, M., et al., *Alkali-activated mortars: Workability and rheological behaviour*. Construction and Building Materials, 2017. **145**: p. 576-587.
40. Snoeck, D. and N. De Belie, *From straw in bricks to modern use of microfibers in cementitious composites for improved autogenous healing—A review*. Construction and Building Materials, 2015. **95**: p. 774-787.
41. Lahmann, D., C. Edvardsen, and S. Kessler, *Autogenous self-healing of concrete: Experimental design and test methods □ A review*. Engineering Reports, 2023. **5**(1): p. e12565.
42. Liu, X., et al., *Carbonation behavior of calcium silicate hydrate (CSH): Its potential for CO<sub>2</sub> capture*. Chemical Engineering Journal, 2022. **431**: p. 134243.
43. Anbu, P., et al., *Formations of calcium carbonate minerals by bacteria and its multiple applications*. Springerplus, 2016. **5**: p. 1-26.
44. Zhang, X., et al., *A novel method to improve the soil erosion resistance with fungi*. Acta Geotechnica, 2022: p. 1-19.

## APPENDIX: RESEARCH RESULTS

### Sidebar Info

**Program Steering Committee:** NCHRP IDEA Program Committee

**Month and Year:** August 2023

**Title:** Development of An Innovative Biomediated Self-Healing Concrete Technology

**Project Number:** 233

**Start Date:** Oct 1, 2021

**Completion Date:** Sep 30, 2023

**Product Category:** New or improved tool or equipment

### Principal Investigator:

**Name, Title:** Xiong (Bill) Yu, Opal J. and Richard A. Vanderhoof professor and chair, Department of Civil and Environmental Engineering, Case Western Reserve University

**E-Mail:** xxy21@case.edu

**Phone:** 216-368-6247

### TITLE:

Innovative Biomediated Self-healing Concrete Technology

### SUBHEAD:

Self-healing microcapsules loaded with fungi agents that efficiently heal wide concrete cracks and prevent water infiltration.

### WHAT WAS THE NEED?

Cracks in concrete structures significantly compromise their durability. For example, cracks are commonly observed in bridge decks at different stages of service, due to early age volume shrinkage, or long term service loads, and climate conditions (i.e., dry-wet cycles, freeze-thaw cycles). Non-structural cracks generally don't pose immediate safety concern. However, they compromise the service life of bridge decks by allowing water and salt ingress that accelerate rebar and concrete corrosion. Bridge deck rehabilitation and replacement is typically the largest share of bridge maintenance cost during the service period of a highway bridge. The large number of bridges and distributed nature of transportation infrastructure makes it difficult to inspect and treat concrete cracks timely with conventional maintenance procedures. Besides, these operations expose highway construction workers to potential safety hazards. Autogenous healing concrete cracks with no need of human intervention, i.e., self-healing concrete, is highly desirable for the longevity of concrete transportation infrastructure.

### WHAT WAS OUR GOAL?

This project aims to conduct proof-of-concept investigation towards developing an innovative fungi-mediated self-healing concrete technology. The innovative self-healing concrete technology aims to extend life of concrete structure with fast and autogenous concrete crack healing.

### WHAT DID WE DO?

The research activities were conducted in these phases. Phase 1 focused on assessing the interactions of fungi with concrete to improve fungi survivability and growth. Promising fungi strains with promising healing performance were identified. Methods were developed to improve the survivability and growth rates of fungi to ensure efficient fungi growth and healing. A scalable production procedure was developed to produce self-healing microcapsules. Phase 2 explored the development of microcapsules to shield the fungi spores. From the experimental trials and observations, the optimal microcapsule recipe was identified. Procedures and equipment to produce microcapsules were developed which features excellent scalability. Phase 3 implemented an experimental protocol to assess the performance of the self-healing agents. Sensitivity study was conducted on the influence of different concentrations of self-healing microcapsules and their



performance with healing cracks in a cement mortar mix with a range of widths. Cracks over 1mm were successfully healed with the fungi-based healing agents.

### WHAT WAS THE OUTCOME?

The fungi self-healing agent successfully healed cracks as wide as 1mm in a cement mortar mix, which is beyond the state of the art in the self-healing technologies. It restores water tightness of concrete surface with hydrophobicity. The self-healing agents can be manufactured with scalable production procedures.

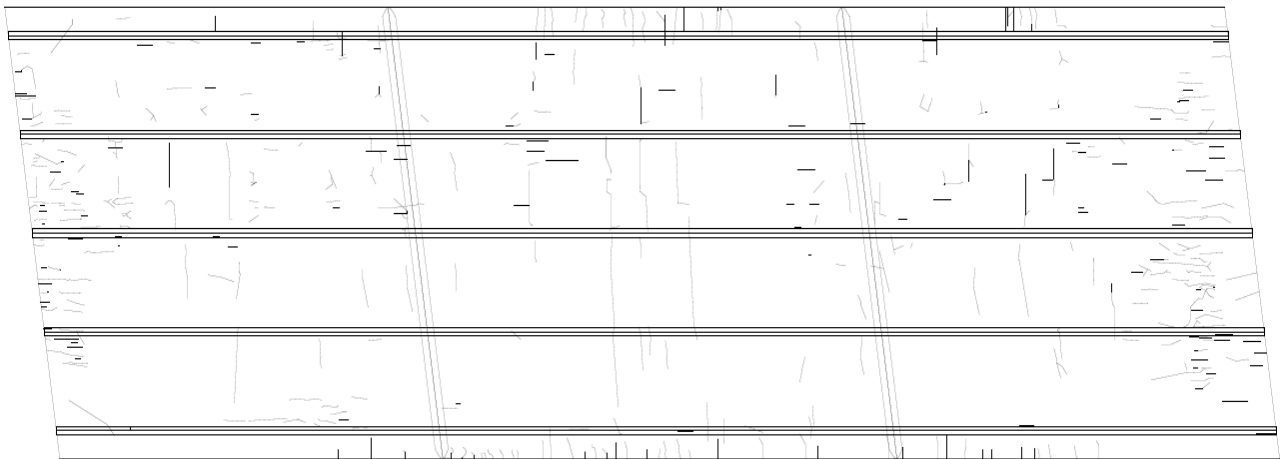
### WHAT IS THE BENEFIT?

This innovative autogenous heal-healing concrete technology will improve the durability of concrete transportation structures, important for sustainability. Reduction of manual maintenance operations for crack sealing will also mitigate the exposure of construction crew to potential safety risks.

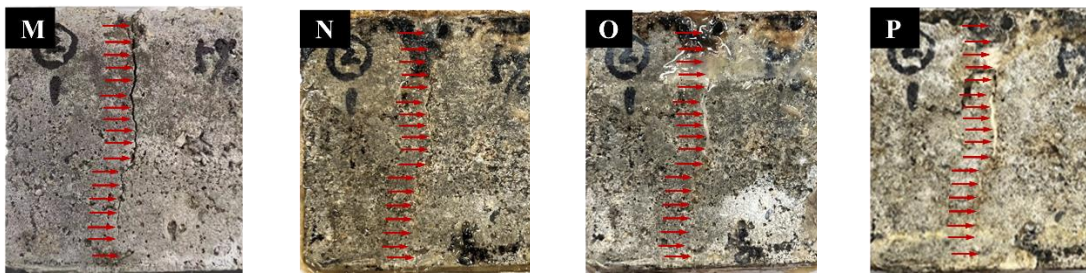
### LEARN MORE

*<Provide link to final report or other pertinent info, such as how to access an online tool.>*

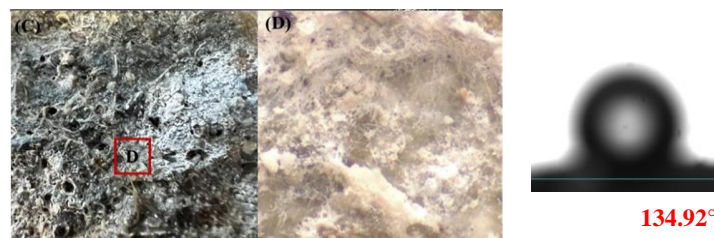
### IMAGES



Schematic illustration of extensiveness of cracks on concrete bridge deck



Autogenous healing of wide crack (>1mm) with developed technology



Observed super hydrophobicity on crack surface treated with self-healing agents

